Development of a Biocompatible Method of Implanting Multi-electrode Arrays for Stable Chronic Deep Neuronal Recording

By

Yihvan Vuong

B.S., Materials Science and Engineering (2003)

Massachusetts Institute of Technology

Submitted to the Department of Biological Engineering
in Partial Fulfillment of the Requirements for the Degree of
Master of Engineering in Biological Engineering

at the

Massachusetts Institute of Technology

September 2004

Signature of Author .....
Department of Biological Engineering
August 6, 2004

Certified by .....
James J. DiCarlo, M.D., Ph.D.
Assistant Professor of Neuroscience
Thesis Supervisor

Certified by .....
Karen K. Gleason, Ph.D.
Professor of Chemical Engineering
Thesis Reader

Accepted by .....
Roger D. Kamm
Director, Master of Engineering Program in Biological Engineering

Development of a Biocompatible Method of Implanting Multi-electrode Arrays for Stable Chronic Deep Neuronal Recording

By

Yihvan Vuong

Submitted to the Department of Biological Engineering
on August 6, 2004 in Partial Fulfillment of the
Requirements for the Degree of Master of Engineering in
Biological Engineering

ABSTRACT

Flexible multi-electrode arrays represent an evolving technology for chronic deep neuronal recording. We focus on developing a biocompatible method of implanting a novel 12-electrode device for long-term recording (weeks to months) in a deep target responsible for object identification, the inferotemporal cortex (IT). Numerous electrodes embedded in a bioerodible polymer matrix composed of 50/50 poly(D,L-lactide-co-glycolide) created an electrode bundle that was sufficiently stiff for insertion into brain tissue, but was expected to become more flexible after polymer degradation. Titanium electrode ports used to house these multi-electrode arrays were successfully designed, constructed, and implanted on a non-human primate as well. These ports were tested for mechanical durability over a course of 6-8 weeks. To evaluate the recording properties of the electrodes, many parameters of the electrode bundle tip were explored and evaluated, including gold-plating, tip cutting (flat cut, angle cut, or individual wire cut), and splaying. Gold-plating lowered electrode impedance and improved signal quality on originally high impedance electrodes. The angle cut and individually cut electrodes were superior to the flat cut ones; they recorded from 6-7 active channels at varying depths during advancement. Splaying, the removal of polymer some distance from the array tip to separate the bundle into individual electrodes, also improved the recording properties in acute experiments. Pending chronic experiments will further reveal 1) the true degradation rate of the array and thus the flexibility restored, 2) the electrode tip characteristics following polymer erosion, and 3) the long-term recording quality and stability of all the electrodes.

Thesis Supervisor: James J. DiCarlo, M.D., Ph.D.
Title: Assistant Professor of Neuroscience

TABLE OF CONTENTS

LIST OF FIGURES

LIST OF TABLES

1 Introduction

1.1 Purpose

One of the primary goals of visual neurophysiology is to understand the neuronal representations that underlie visual object recognition. In the brain of the non-human primate, these representations are thought to be carried in the population pattern of neuronal activity in a neocortical region located deep in the skull – the inferotemporal cortex (Fig. 1). Thus, a fundamental research goal is to understand how these patterns of neuronal activity are caused by retinal images of objects, and how they are modified by visual experience with such objects.

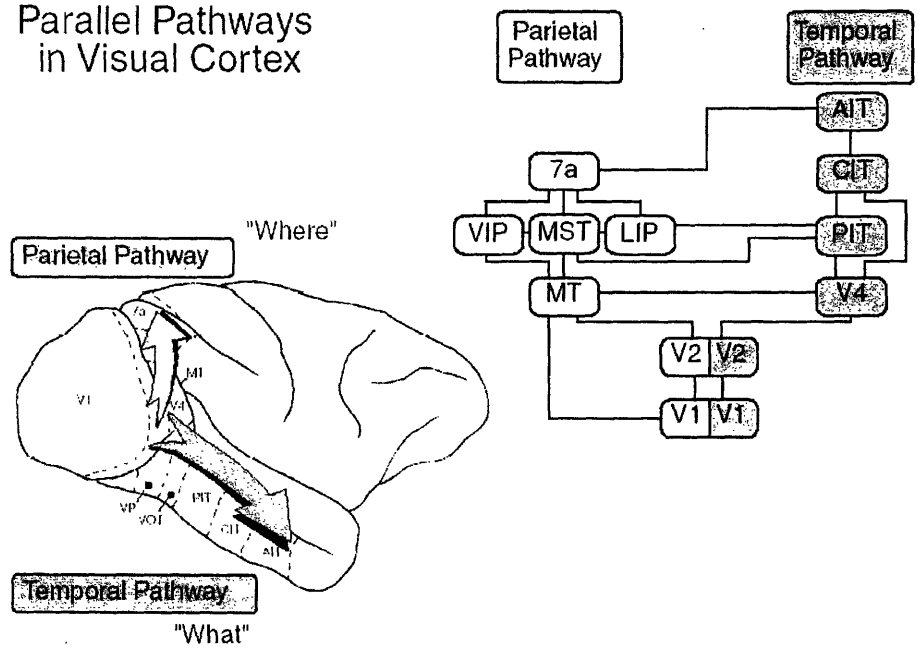

Figure 1. Diagram depicting the visual processing centers of the cerebral cortex. Information from retinal images propagates along two streams from the primary visual cortex – the parietal pathway and temporal pathway. We are interested in the temporal stream that leads to the anterior inferotemporal cortex, believed to be responsible for object identification.

1.2 Problem

To further this goal, we aim to develop neuronal recording electrodes that can be implanted in deep brain tissue and reliably record neuronal signals for long periods of time, such as weeks or months. The electrodes currently used to study neuronal responses in the inferotemporal cortex (IT) can only be employed in acute recording experiments, which run approximately 3-6 hours for each session. Individual neurons typically remain isolated for 30-60 minutes. In between experiments, electrodes are implanted, removed, and then re-implanted. As a result, there is absolutely no ability to record from the same neuron upon reinsertion and no ability to study the same neuron for long periods of time.

Our first objective is to extend this recording time, so that signals from the same locations and perhaps the same neurons can be recorded from for longer. In theory, chronic electrodes are superior to acute electrodes because they 1) can gather much more data from each neuron, 2) can monitor long-term changes in the response of each neuron, and 3) are much more economical in regards to test subjects and time. Less time is needed to set up for recording since the electrodes are already inserted. Chronic implants also cost less since they are not constantly being replaced, which happens often for acute electrodes. The ability to chronically record from deep areas would be a major advance in allowing us to understand how visual object information is organized and stored in the IT cortex.

Our second related objective is to increase the efficiency of data acquisition from neurons in IT. The current method of deep neuronal recording utilizes only a single electrode at a given time. It is desired to increase the number of electrodes inserted into brain tissue. A higher throughput electrode device is advantageous because it 1) increases the number of neurons that can be detected and recorded from at a given time and 2) provides a more comprehensive representation of IT population pattern of activity through simultaneous data acquisition.

2 Background

2.1 Electrode Mechanical and Material Specifications

There are several mechanical and materials engineering issues regarding neuronal recording from deep brain tissue structures such as IT. The first engineering concern involves the stiffness of the electrode. For IT recording in the non-human primate, the electrode must travel 35-40mm from the skull surface upon insertion to reach the IT cortex (Fig. 2). It is necessary for the electrode to have the right mechanical stability in order to track straight toward the recording region and avoid flexing. A sufficiently stiff electrode will ensure that the device is placed in or near the desired recording site. Once positioned in the deep brain region (e.g. IT), however, there is also a need for the recording electrode to possess some degree of flexibility so that it may "float" within the brain matter. This flexibility allows the electrode to settle in the tissue and shift with the brain as it naturally pulses and moves within the skull. This may lead to an improvement in signal stability because the electrode remains embedded in the same location instead of resisting and traveling to other tissue areas. We hypothesize that stiff electrodes do not yield to the small movements of soft tissue, and thus the electrode migrates as the brain pulses.

An electrode's ability to submit to these physiological movements can also potentially reduce the damage inflicted on neurons, glial cells, and blood vessels during and after insertion. When a stiff electrode is implanted, it is sufficiently rigid and sharp enough to puncture through cells and blood vessels. A flexible electrode may have more freedom to maneuver between cells and around small blood vessels. This decrease in invasiveness can consequently lead to a lower level of acute and chronic inflammation; less injury results in fewer astrocytic cells, multinucleated foreign-body giant cells, and other injury-responsive immune cells encasing the foreign electrode. Although this reduction in inflammation might not be maintained throughout the lifetime of the implant, it can potentially improve and uphold the recording quality of the

electrode, a characteristic that is particularly sensitive to organic material attaching to the electrode tip.

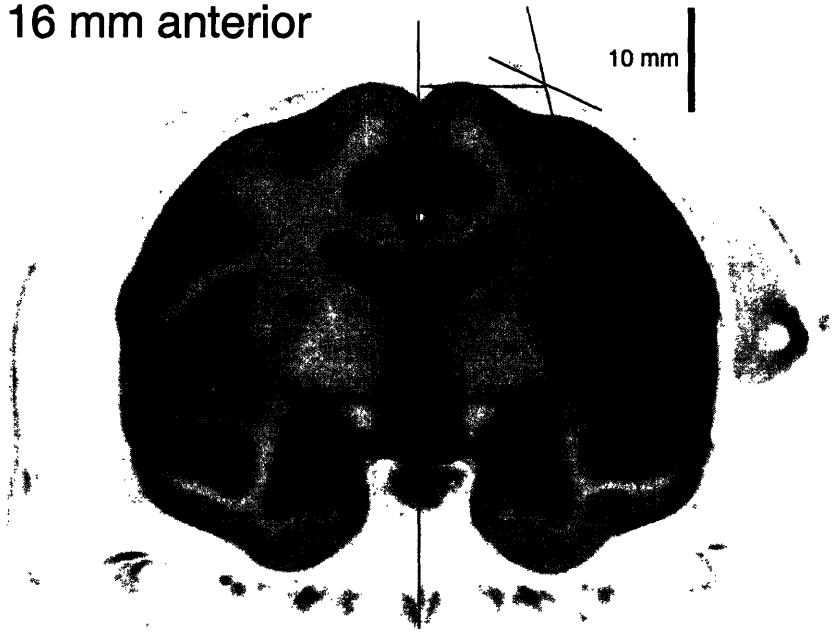

Figure 2. Coronal magnetic resonance image of a rhesus monkey brain. The track taken to reach the anterior inferotemporal cortex is marked by the red line. The electrode must enter through the dorsal surface approximately 12mm lateral and 16mm anterior, and travel 35-40mm to enter IT.

The second engineering concern involves the biocompatibility of the chronically implanted electrode. In acute experiments, the electrode is removed after recording, reducing the risk of complications such as infection and immune response. In chronic studies, however, the electrode is permanently placed and thus biocompatibility of the electrode becomes a critical issue. Not only is it desirable to prevent a significant host reaction towards the foreign implant, it is also vital to keep the recording device clear from immune cells in an effort to maintain signal quality. Thus, selecting a biocompatible and bio-inert electrode material is essential. Biocompatibility is defined as "the ability of a material to perform with an appropriate host response in a specific application."[1] Furthermore, the insulation for the electrode must also be sufficiently biocompatible because its entire surface area interacts with the surrounding tissue. In an effort to reduce the potential for inflammation, the surface area that the insulation contacts the tissue should be minimized. To lessen the invasiveness of the insertion procedure and the resulting inflammation, the electrodes should also be manufactured as thin and small as possible. The ultimate goal is to create a multi-electrode array that can be left inside the brain for an extended period of time on the scale of weeks or months. Eventually, the electrode would be able to reside in the brain for months or years without inducing a significant host reaction.

---

[1] Williams D.F. *Definitions in Biomaterials. Proceedings of a Consensus Conference of the European Society for Biomaterials*, Chester, England, March 3-5 1986, Vol. 4, Elsevier, New York.

Because the electrode is not removed during chronic experiments, the insertion area must also always be kept clean from bacteria and other infectious agents. The skull opening must be protected from the hazards of infection. If compromised, this area can easily jeopardize the experiment and may be detrimental to the test subject.

2.2 Current Electrode Materials

Certain materials are preferred over others for constructing electrodes used in recording and micro-stimulation experiments. Platinum, iridium, rhodium, palladium, and gold are commonly used because these materials have high electrical conductivity, low chemical reactivity, and high resistance to corrosion. These metals undergo chemical dissolution to a much lesser extent and thus are more bio-inert than other metals. Platinum is a soft metal often used in neural prostheses and cardiac stimulation applications (Ratner et al., 1996). This metal can also be combined with iridium to produce alloys with higher mechanical strength. Platinum/iridium alloys are often used for intracortical stimulation where piercing through the thick dura covering of the brain is necessary before reaching the cortex.

There are also a variety of insulators currently used: medical-grade silicone rubber, Teflon, polyimide, and epoxy. Key specifications for the insulator include providing pinhole-free coatings, bio-inertness, and good adherence to the electrode conductor (Ratner et al., 1996). Insulation is required because only the tip should have high electrical conductivity. Otherwise, the electrode would detect neuronal signals along the entire length of the wire, making pertinent multi-unit and single-unit activity very difficult to isolate. The locations of these specific neurons would also be nearly impossible to determine.

The electrodes made at present by the DiCarlo lab consist of platinum/iridium bare wire 0.003 inches or 76μm in diameter (A-M Systems) partially inserted into 32-gauge regular wall #316 stainless steel shafts (229μm OD and 102μm ID; Vita-Needle). The exposed platinum/iridium wire is electrochemically etched using a 5V source and sodium cyanide solution until the tip is sharpened to approximately 1μm in diameter. The wire portion is then insulated with glass from the shaft/wire interface to the etched tip, leaving approximately 40μm of the tip exposed. Finally, polyimide tubing (274μm OD and 249μm ID; Microlumen) is inserted over the other end of the stainless steel shaft down to the glass insulated platinum/iridium wire. This serves as insulation for the rest of the electrode. Loctite 420 instant adhesive is used to adhere the tubing to the steel shaft and glass insulation, forming one continuously insulated electrode. Specifications for the electrode include an impedance range between 0.1-1Mohm at 1 kHz and the potential to stimulate with μAmp range current pulses through the electrode.

It should be emphasized that these electrodes are single stiff electrodes used for acute experiments; they have never been applied to chronic studies. These electrodes possess ample mechanical stiffness to track straight into the brain. However, they lack the desired flexibility to remain embedded in the same tissue area. Moreover, these electrodes are insulated with glass which during insertion, can fragment when encountering obstacles such as blood vessels. The glass shards remain embedded in the tissue and are incompatible with the host environment. During microstimulation, the glass insulation also disintegrates while μAmp current pulses are applied through the electrode, posing as a significant hazard to the test subject.

These single electrodes are used in conjunction with relatively large head chambers (0.95 inch or 24.13mm in diameter; Crist Instruments Co., Inc.). The chamber is surgically fixed on the monkey's skull, requiring a fairly large craniotomy. Due to the large site of exposed dura and brain tissue, the chamber poses as a significant risk for infection. Once implanted, the chamber interior must also be cleaned often, approximately three times a week. Although popular for deep brain recording, this type of electrode/chamber system can certainly be improved upon.

2.3 Electrode Scalability Specifications

Our goal of increasing the data acquisition ability of the electrodes essentially involves inserting multiple electrodes into the same area. This can be achieved through two methods by 1) increasing the number of electrodes per recording device and 2) increasing the number of recording devices implanted into the brain.

The short-term goal of scaling up electrode recording capability involves implanting more electrodes into the brain. This requires a suitable connector that can house numerous electrodes simultaneously. The long-term goal of simultaneous data acquisition includes placing as many as 50 of these multi-electrode devices on the skull. For the electrode arrays to be scalable, they must also be as thin as possible. In addition, the mounting head on the skull surface to which the floating electrodes are attached to must be small and compact for each electrode array. Ideally, these mounting heads would be less than 5mm in diameter. A design that allows 1-2mm of adjustment of electrode depth would be best for optimizing the neuronal recording, allowing different layers of neuronal tissue to be sampled. However, all these goals must be balanced against an increase in implant size and the resulting decrease in scalability.

2.4 Current Multi-electrode Technology

Several devices have been created to record more neuronal signals simultaneously. One example is the tetrode, a flexible electrode composed of four wires helically wound together. They have been successfully employed to record in the hippocampus of rats (Fig. 3), a region located below the neocortex (Wilson and McNaughton, 1993; Jeantet and Cho, 2003). Tetrodes have also isolated single units or individual neurons from multi-unit activity in the striate or primary visual cortex of cats (Gray et al., 1995). In these experiments, recording from deep brain tissue was achieved, but with much smaller test subjects. The distance of travel was much shorter than the 35-40mm necessary for deep brain recording in non-human primates.

For larger test subjects like non-human primates, tetrodes have been implanted to study the primary visual cortex (Mechler et al., 2002; Aronov et al., 2003). However, these animals were under deep anesthesia during the course of the experiment. In addition, the experiment was acute, and the animal was sacrificed 5 days into the experiment. Because the primary visual cortex is on the surface of the brain, these tetrodes also traveled a much shorter distance (e.g. 5mm) than the 35-40mm necessary to reach IT. Tetrodes have recorded from brain structures that are located at a similar depth to IT as well. Implanted tungsten/nichrome tetrodes have successfully recorded neuronal signals from the perirhinal cortex (Fig. 3), a region in anterior medial IT cortex, in male rhesus monkeys (Erickson et al., 2000; Erickson and Desimone, 1999). However, these tetrodes were semi-chronic and could remain implanted for only one month. The tetrodes also required a 30-gauge stainless steel telescoping guide tube for mechanical support.

The macroscopic tube with an approximate diameter of 305μm is very large for insertion into deep brain regions and can significantly distort the tissue during tetrode advancement.

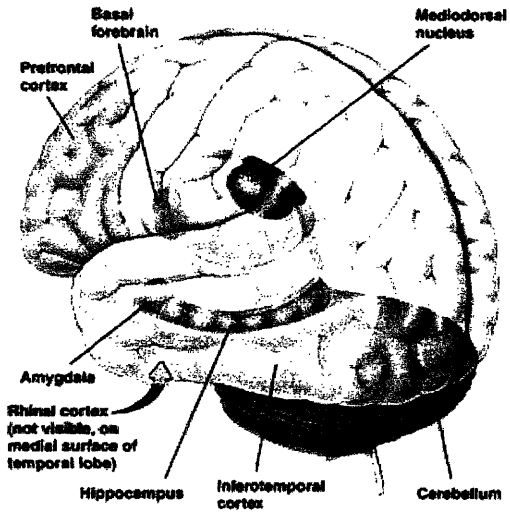

Figure 3. Schematic illustrating different regions of the brain. As discussed in this section, the rhinal cortex, hippocampus, and inferotemporal cortex are deeper areas that have been explored using tetrode and multi-electrode array technology. Recording from the rhinal and IT cortex constitute deep brain recording.[2]

Other multi-electrode devices have been produced for chronic recording in larger test subjects. More than a year of recording from the primary visual cortex of a marmoset was achieved using a 64-electrode array (Porada et al., 1999). While the electrodes in this study were implanted indirectly via a distant trepanation to reach V1 area, it should be reemphasized that the primary visual cortex is located on the surface of the cerebral cortex and can be directly accessed with relative ease compared to IT. This study was moderately invasive, requiring a syringe cannula 0.5mm in diameter to house the flexible Ni-Cr-Al alloy wires during and after insertion. This device was also rather bulky; only one device could be implanted on the marmoset at a given time. However, their success with stable chronic recording suggests potential of these flexible electrodes to be excellent recording devices.

Chronic recording in awake macaque monkeys have been achieved using high-density microwire arrays as well (Nicolelis et al., 2003). Five different motor cortex areas (M1) were recorded from over a period of 3-4 weeks after implantation. However, these arrays were designed for shallow brain recording (e.g. 5-10mm). A microelectrode drive containing 42 electrodes with 14 independent drive mechanisms have also been developed to record from awake and freely moving or chaired macaque monkeys (Wilson F. et al., 2003). These electrode drives can be

[2] See URL: http://www.driesen.com/ memory_in_the_brain.htm Accessed 7.27.2004

implanted up to six months at a time, but can only record from the dorsolateral prefrontal cortex and hippocampus. In summary, previous work suggests potential for chronic recording, but development of chronic electrodes specifically for deeper targets (i.e. IT) is rather limited.

2.5 General Approach

The first goal in this project is the development of a biocompatible method of inserting multiple electrodes into a deep target and leaving flexible electrodes in place. We aim to create multi-electrode arrays that are stiff during implantation into brain tissue, but become more flexible after they are positioned. This method will not require invasive devices such as cannulas during insertion. These multi-electrode arrays will be developed with an eye towards scalability by keeping them as thin as possible. The second aim is to compare the recording properties between the single stiff electrodes currently used by the DiCarlo lab and the flexible electrodes through acute experiments in rhesus monkeys. Once the electrodes and insertion method are optimized, the third aim is to test a prototype of this device for weeks of recording from monkey IT and document the degree of recording stability.

2.6 Criteria for Success

This is a very challenging problem to completely resolve in the time span of one year. The main goal is to begin the development of these electrodes so that one day they may replace the current single probes. Multi-electrodes will be designed and fabricated to meet desired specifications. All elements regarding their insertion and implantation will be devised as well. This includes aspects such as electrode ports implanted on the skull to house the electrodes and driving devices for smooth loading of the electrodes during acute and chronic implantation. This project will be deemed successful if 1) a biocompatible method of inserting these arrays is developed, 2) the electrode ports are successfully designed and implanted, 3) the electrode arrays demonstrate recording potential through acute experiments, and 4) chronic experiments utilizing these arrays are initiated to observe recording quality and stability over a period of 2-3 months.

3 Theory

Flexible electrodes have been conjectured to be superior to stiff electrodes in terms of recording stability and tissue injury because they are more adaptive to their local environment. Previous chronic studies using tetrode and microelectrode technology have employed flexible, instead of stiff, electrodes for recording (Erickson et al., 2000; Porada et al., 1999). The main drawback of flexible electrodes is they, by definition, lack mechanical stiffness. In this project, we focus on creating an electrode that is mechanically stiff during insertion but becomes flexible after implantation. Such an electrode would be rigid enough to penetrate brain tissue, but would gradually lose its stiffness. The flexibility gained would then allow the electrode to settle in the brain.

A single flexible electrode usually deforms and buckles when traveling through dura and into the IT cortex. For deep brain recording, this electrode must be reinforced mechanically to increase its stiffness. Several solutions considered were 1) inserting a bioerodible cannula with an array of unmodified electrodes, 2) using a longer stainless steel guide tube to aid the electrode in tracking straight, and 3) combining many flexible electrodes to make one mechanically stiff

electrode array. The first option is similar to the method proposed by Porada et al. and is highly invasive for deep brain recording. The macroscopic cannula can extensively damage tissue during advancement of the electrode into IT. The second option of using a guide tube encounters the same problems as the cannula. Current guide tubes are already inserted 15-20mm into tissue to assist the electrode in straight tracking. Increasing that could damage more tissue surrounding IT. Therefore, to accomplish our goal we explore the third option and integrate numerous flexible electrodes with a bioerodible polymer to enhance the probe's total mechanical stiffness. The electrode array will be much thinner than a cannula or guide tube. A "bioerodible polymer" is defined as "a water-insoluble polymer that is converted *under physiological conditions* into water-soluble material(s) without regard to the specific mechanism involved in the erosion process."[3] This erosion process includes physical processes such as dissolution of the material and chemical processes such as polymer backbone cleavage.

3.1 Electrode-Polymer System

The electrode array consists of multiple flexible electrodes embedded in a polymer matrix. These individual wires reinforce each other and combine their rigidity, increasing the overall mechanical stiffness of the probe. The number of electrodes present directly influences the stiffness of the bundle and its resistance to buckling. However, the force and thus the number of wires needed to penetrate the brain are unknown. A bundle composed of five electrode wires may be insufficient, but one made of ten wires may be satisfactorily stiff. To design a multi-electrode array that is suitably resistant to buckling, we model the stiffness to be near the stiffness of current single electrodes. These electrodes have been proven experimentally to track straight into the brain without buckling during insertion. While this type of electrode may be overly stiff, it provides us with an upper limit of what constitutes sufficient rigidity.

The chosen polymer does not add much mechanical strength to the probe; its inherently low tensile modulus compared to metals (Table 1) and the amount we hope to coat onto an electrode does not significantly increase the critical load for buckling. Here we present mathematical support for our logic using a fixed-free column buckling equation. This formula assumes one end to be free and the other to be cantilevered, an imitation of what happens during electrode insertion. One end of the electrode is fixed while the other is free to move in any direction. The critical load or force needed for buckling is represented by:

$$P_{cr} = \frac{\pi^2 EI}{4L^2}$$

where E is the elastic or Young's modulus, L is the length of the beam, and I is the moment of inertia for the beam. I is dependent on the shape of the beam, and for this case we use two examples – a solid cylinder and a hollow cylinder. This is represented by:

$$I_{solidcylinder} = \frac{\pi D^4}{64}$$

[3] Ratner et al., Biomaterials Science: An Introduction to Materials in Medicine. Elsevier Science: 1996. p.66

$$I_{hollowcylinder} = \frac{\pi}{64}\left(OD^4 - ID^4\right)$$

where D is the diameter of the cylinder, OD is the outer diameter of the hollow cylinder, and ID is the inner diameter of the hollow cylinder. Let us consider the case for a single flexible nichrome wire. The diameter of this bare nichrome wire is 25μm, and the elastic modulus is $2.0\text{x}10^{11}$ Pa or N/m^2. The moment of inertia (for a solid cylinder) is therefore

$$I_{solidcylinder} = \frac{\pi\left(2.5\times10^{-5}m\right)^4}{64} = 1.9\times10^{-20}m^4$$

Assuming the length of the wire is 40mm for the electrode to travel into IT, the resulting critical load for buckling is

$$P_{cr} = \frac{\pi^2\left(2.0\times10^{11}\frac{N}{m^2}\right)\left(1.9\times10^{-20}m^4\right)}{4(0.04m)^2} = 5.9\times10^{-6}N$$

Next, we want to determine how much the critical load for buckling will increase if a polymer coat is added to the electrode. The polymer coat is generously estimated to be 20μm thick, close to the bare diameter of the electrode. The tensile modulus for the polymer is also approximated to be $3.5\text{x}10^9$ N/m^2. The moment of inertia for a hollow cylinder (just the polymer coat) and the critical load for buckling are calculated to be

$$I_{hollowcylinder} = \frac{\pi}{64}\left[\left(6.5\times10^{-5}m\right)^4 - \left(2.5\times10^{-5}m\right)^4\right] = 8.57\times10^{-19}m^4$$

$$P_{cr} = \frac{\pi^2\left(3.5\times10^{9}\frac{N}{m^2}\right)\left(8.57\times10^{-19}m^4\right)}{4(0.04m)^2} = 4.6\times10^{-6}N$$

For the polymer coated nichrome wire, the critical load for buckling is simply the sum of the P_{cr} for the solid nichrome wire and for the polymer tube, which is $1.05\text{x}10^{-5}$ N. The polymer coat has made the electrode almost twice as resistant to buckling as a bare electrode.

This critical load for buckling is compared to the stiff electrodes currently used by the DiCarlo lab. These electrodes employ 32-gauge stainless steel #316 tubing as the main body of the electrode. Without including the polyimide insulation and taking this as the lower limit of electrode stiffness, the P_{cr} for the electrode is calculated. With an OD of $2.29\text{x}10^{-4}$ m and an ID of $1.02\text{x}10^{-4}$ m, the moment of inertia for the tube is calculated to be $1.3\text{x}10^{-16}$ m^4. The modulus for #316 stainless steel is $1.9\text{x}10^{11}$ N/m^2, and thus the critical load for buckling is $3.8\text{x}10^{-2}$ N. Thus, the current electrodes are approximately 3,600 times more resistant to buckling than a

single polymer coated flexible wire. In terms of how flexible the polymer coated nichrome wire still is compared to the stiff electrode, the polymer coat does not seem to significantly increase the mechanical stiffness of the wire.

We then calculate how much more resistant an electrode bundle would be to buckling compared to the polymer coated flexible electrode and single stiff electrode. Let us assume that in an electrode bundle there are 12 electrode wires stacked compactly together and are unable to slide pass one another. This would be similar to polymer bonding all the wires together to form one solid bundle. There are two limiting cases. The lower limit case is composed of all 12 wires packed infinitely tight without any gaps between separate wires. The cross-sectional area of this bundle would be the sum of all the individual wire areas. The upper limit case is composed of the 12 wires compactly packed into a circular bundle, but still with small spaces between the electrodes. The cross-sectional area of this bundle would be larger than if the electrodes were infinitely packed together. In both cases, we neglect the polymer used to hold the electrodes together; we assume that there is significantly more wire than polymer in the composite.

For the lower limit case, the total area is 12 times the cross-sectional area of a single electrode or 5.9×10^{-9} m^2. The diameter of this "solid" bundle is 8.66×10^{-5} m. The moment of inertia calculated for a solid cylinder is 2.76×10^{-18} m^4, and the resulting critical force for buckling is 8.5×10^{-4} N. In the upper limit case, we include the insulation of the nichrome (38μm diameter) and assume the entire diameter is composed of electrode wire. The stacking arrangement for the bundle results in a diameter that is approximately 3.5 wire diameters or 1.33×10^{-4} m. The moment of inertia for a solid bundle of this layout is calculated to be 1.54×10^{-17} m^4, which results in a critical load for buckling of 4.7×10^{-3} N. From these calculations, we gather that these 12 wire electrode bundles have a critical load for buckling in the range of 8.5×10^{-4} - 4.7×10^{-3} N. This is between 80-440 times more resistant to buckling than a single polymer coated wire and only about 8-45 times weaker than current stiff electrodes. Clearly, the electrode bundles are more similar in stiffness to current electrodes than the single coated flexible electrodes.

The polymer only serves as a bonding agent by holding the individual wires together in a polymer-electrode composite and keeping them from flexing during insertion into the brain. After the electrode array is implanted, however, the bioerodible polymer contacts the aqueous environment and gradually degrades. Following complete breakdown of the biomaterial, each electrode's intrinsic flexibility is restored, allowing it to pulse with the brain and adjust to its natural movements. At this stage, the electrode bundle can no longer be modeled as one large solid cylinder, but instead 12 smaller individual cylinders. The critical force for buckling and thus stiffness becomes significantly lower as well since these wires are no longer linked together.

The number of electrodes in a bundle will ultimately also depend on available electronic connectors; all electrode wires will be fixed to a single multi-port connector in an effort to optimize scalability. Although the number of electrodes needed to generate sufficient stiffness is unknown, designing the bundle to be similarly stiff as the electrodes that have already been proven to work is a good strategy. Furthermore, these calculations only provide an estimation of the desired stiffness. Even for a 12 electrode bundle the stacking can be varied in numerous ways that affect the resulting buckling resistance. If the electrodes are embedded in additional

polymer and consequently packed more loosely, the resistance will change because the stacking arrangement is altered. Realistically, once the electrode array enters deeper into brain tissue the situation for buckling also changes because the medium is different. Instead of the beam being surrounded by air, it is embedded in thicker brain tissue. Tuning the stiffness with the number of electrodes must also be balanced with scalability; 20 electrodes loosely packed in a polymer matrix may not buckle during array insertion, but may be over 400μm in diameter and much thicker than desired.

This electrode array fulfills all of the mechanical specifications previously stated for an electrode device. It provides adequate stiffness for insertion while becoming more flexible after implantation. Stiff electrodes alone are unable to change their degree of flexibility because of their metal shafts. Single flexible electrodes, uncoated or coated with polymer, do not possess sufficient stiffness to penetrate tissue. Thus, this flexible multi-electrode array provides a satisfying solution to all problems at hand.

Table 1 Mechanical Properties of Some Bioerodible Polymers Compared to Electrode Metals

Polymer	**Molecular Weight**	**Tensile Strength [MPa]**	**Tensile Modulus [MPa]**
Poly(glycolic acid)[a]	>100,000	69+	6900
Poly(lactic acid)[b]	100,000	50	2700
	300,000	48	3000
Poly(ε-caprolactone)[b]	44,000	16	400
Poly(SA-HDA anhydride)[b]	142,000	4	45
Poly(ortho ester) DETOSU: t-CDM: 1,6-HD[b]	99,700	20	820
Metal	**Type**		
Platinum[c]	n/a	125-300	$1.7x10^5$
Iridium[c]	n/a	550-1200	$5.28x10^5$
Nichrome Alloy[c]	80-20	400-660	$2.0x10^5$
Stainless Steel[d]	Type 316	1070-1275	$1.9x10^5$

(a) Specifications from Birmingham Polymers, Inc.
(b) Specifications from Ratner et al., Biomaterials Science, 1996.
(c) Specifications from www.goodfellow.com
(d) Specifications from www.a-msystems.com

3.2 Polymer Selection

Many factors must be taken into account when selecting a polymer with the appropriate erosion characteristics. The size and geometry of the electrode bundles as well as polymer-electrode surface interactions play critical roles in the degradation rate of the polymer. The hydrophobicity, crystalline structure, hydrolytic cleavage rate, degradation products, and processing parameters of the polymer are also significant factors that contribute to the erosion rate. The implantation site affects the degradation rate as well since areas of the body have diverse local environments that vary in pH, enzyme contact, hydrolytic exposure, and mechanical stress.

For the multi-electrode array, we aim to use bioerodible polymers that completely degrade within 1 week following implantation. Since the brain is approximately 75% water, there is no

difficulty for the polymer coated bundle to contact water. However, even with a constant exposure to water, the degradation mechanism and time varies depending on the polymer. The products from polymer breakdown must also be biocompatible since they will reside in the brain for a period of time before being cleared by the immune system.

Polyanhydrides, polycaprolactones, poly(ortho esters), poly(lactic acid), and poly(glycolic acid) are a few types of polymers that are hydrolytically unstable. These polymers can degrade physically either through bulk erosion or surface erosion and can degrade chemically through bond cleavage (Table 2). In bulk erosion, the rate of water penetration into the solid polymer is greater than the rate of polymer transformation into water-soluble materials. The actual erosion occurs after the majority of the polymeric material has taken up water. This occurs for many hydrophilic polymers because, due to their water-loving nature, there is little resistance against water infiltration. Most hydrophobic polymers, however, undergo surface erosion. In surface erosion, the rate of water penetration into the solid polymer is much less than the rate of polymer transformation into water-soluble materials. Erosion does not occur throughout the polymeric material simultaneously, but only on the surface instead. Over time the material becomes thinner and smaller, but without the immediate loss of structural integrity that occurs in bulk erosion. For our purposes, a polymer that undergoes bulk erosion would be optimal, since the rapid loss of polymer integrity would allow the multi-electrode array to more quickly regain flexibility.

Crystallinity is another factor that affects how quickly the polymer erodes. A highly crystalline polymer has more densely packed chains and provides fewer pores for water infiltration. Poly(glycolic acid) is a highly crystalline polymer and is very difficult to dissolve in solvents; however, the polymer still degrades fairly rapidly due to its high hydrophilicity. Poly(L-lactic acid), a semi-crystalline polymer, has amorphous regions in which water can penetrate and consequently degrade the polymer's crystalline regions. Poly(D,L-lactic acid), the racemic form of poly(lactic acid), has the same hydrophobicity as poly(L-lactic acid), but is much easier to degrade because of its amorphous form and thus high water penetration between the loosely packed polymer chains.

All of the bioerodible polymers listed in Table 1 degrade from hydrolytic cleavage of backbone linkages between monomers (Ratner et al., 1996). However, different bonds also have intrinsically varying cleaving rates even though they degrade through the same mechanism. For example, anhydride bonds tend to hydrolyze faster than ester bonds, and ester bonds tend to hydrolyze faster than amide bonds. Amide bonds also tend to hydrolyze faster than ether bonds. This is an intrinsic characteristic of the bonds and affects the erosion rate. A short summary of the critical properties of polymers that affect degradation kinetics is shown below (Table 2).

Initially, polyanhydrides seem to be optimal polymeric materials due to their particularly rapid degradation rates; aliphatic polyanhydrides tend to degrade within days. However, the sensitive hydrolytic nature of these polymers is difficult to control after fabrication; the excess polymer and coated electrodes must be very carefully stored to prevent premature degradation. We also hope to reuse these polymer coated electrodes for multiple acute experiments in the initial phase of testing similar to how the current stiff electrodes are being used. This will allow us to document the stability of the prototype electrodes between experiments and will be much more

economical in regards to fabrication labor and time. Thus, complete degradation in such a short time period is not ideal, at least for initial experiments.

Table 2 Properties of Several Bioerodible Polymers that Affect Degradation Rate

Polymer	Susceptible Bonds	Structure	Water Preference	Erosion Type
Poly(glycolic acid)	Ester	Highly Crystalline	Hydrophilic	Bulk
Poly(ε-caprolactone)	Ester	Semi-crystalline	Hydrophobic	Enzyme-mediated Surface
Poly(L-lactic acid)	Ester	Semi-crystalline	Hydrophobic	Surface
Poly(DL-lactic acid)	Ester	Amorphous	Hydrophobic	Bulk
Poly(ortho ester)	Acid-sensitive Ester	n/a	Hydrophobic	Surface
Polyanhydride	Anhydride	n/a	Hydrophobic	Surface

The importance of releasing exceptionally biocompatible products when implanted in the brain led us to focus on poly(glycolic acid) and poly(lactic acid). These polymers and their degradation properties have been widely investigated in the last two decades. Poly(glycolic acid) or PGA and poly(lactic acid) or PLA are polyesters that degrade moderately fast but slower than polyanhydrides. PGA and PLA are fabricated from glycolide and lactide dimers, respectively, using ring-opening polymerization (Fig. 4).

PLA exists in several stereoisomeric forms – L-PLA, D-PLA, and D,L-PLA. L-PLA and D-PLA are both semi-crystalline materials. The optical isomer D,L-PLA is a racemic mixture that is a by-product of polymer synthesis and is an amorphous polymer. Hydrolysis of the L-PLA optical isomer yields L(+) lactic acid, which is a compound naturally present in the body. Products from PLA hydrolysis are incorporated into the citric acid cycle and excreted as water and carbon dioxide through respiration. PGA degrades by random hydrolysis and by non-specific esterases and carboxypeptidases (Williams, 1979). These products are subsequently excreted in the urine or converted into other metabolic compounds in the citric acid cycle.

L-PLA has been utilized in orthopedic devices (e.g. bone screws) due to its semi-crystalline nature and its relatively high mechanical strength. D,L-PLA is better suited for drug delivery systems than orthopedic devices because it has relatively low mechanical strength, and its amorphous monophasic nature allows for uniform drug release. PGA has been extensively used in the suture industry and has been sold commercially under the trade name Dexon since 1970. In addition, these polymers have been employed in the making of brain implants, such as devices that release chemotherapeutic agents. Many studies have examined the degradation rates and biocompatibility of PGA, PLA, and PLA-PGA copolymers (Miller et al., 1977; Fournier et al., 2003). Bioerodible microspheres prepared from poly(D,L-lactide-co-glycolide) have been implanted into rat striatum for periods ranging from 24 hours to 2 months and have been found to be biocompatible with the brain tissue (Veziers et al., 2001). Poly(D,L-lactide-co-glycolide) microspheres implanted into rat brain have also been examined for gliotic responses; the results indicated that minimal reaction occurred reaching a peak after one week and decreasing subsequently after one month of implantation (Emerich et al., 1999). This study also concluded that the majority of polymer disappeared between one and four weeks. Erosion studies of poly(D,L-lactide-co-glycolide) rods (300-500μm in diameter) conducted *in vitro* using simulated

and goat cerebrospinal fluid led to the conclusion that the polymer rods degraded within 20 days (Kou et al., 1997). This study also involved implanting these rods into rat brain. The rods were found to be well tolerated by the tissue, and the majority of the polymer degraded after 28 days.

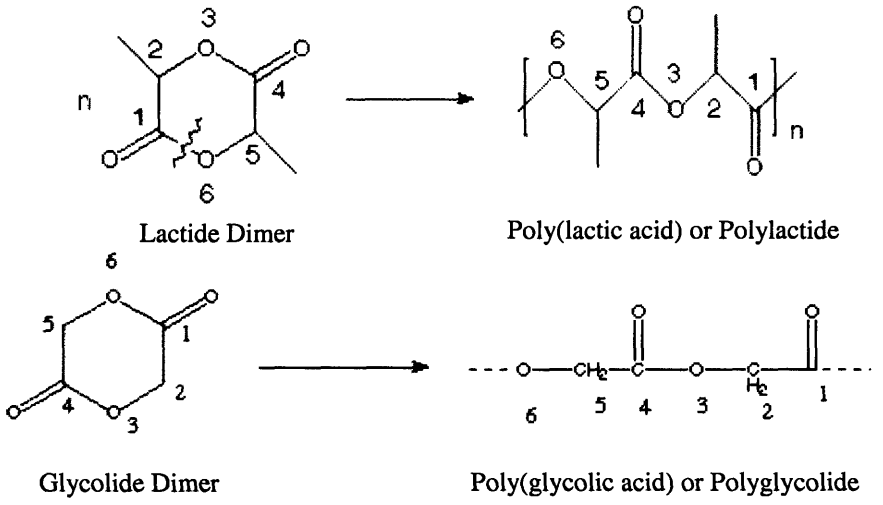

Figure 4. Ring-opening polymerization of lactide dimers to produce PLA and glycolide dimers to produce PGA, respectively. Both polymers are hydrolyzed through their ester bonds and release products that are either incorporated into a metabolic process or excreted.[4]

From these results, we chose to apply a 50/50 polymer blend of poly(D,L-lactic acid) and poly(glycolic acid) to the multi-electrode array. The majority of this copolymer undergoes bulk erosion due to rapid degradation of the amorphous D,L-PLA regions, allowing the array to rapidly regain its flexibility. It also completely erodes away in 3-6 weeks, which falls within the range of our specification. This copolymer can be tuned through its molecular weight to adjust degradation time; a higher molecular weight leads to slower disintegration of the polymeric material. This copolymer has also been proven to be biocompatible with brain tissue. Some general physical and mechanical properties of PLA and PGA homopolymers and their copolymers are indicated below (Table 3).

Table 3 Physical and Mechanical Properties of PLA and PGA Homopolymers and Polymer Blends[5]

Polymer	50/50 DL-PLG	65/35 DL-PLG	75/25 DL-PLG	DL-PLA	L-PLA	PGA
Molecular Weight	40,000-100,000	40,000-100,000	40,000-100,000	40,000-100,000	>100,000	>100,000
Inherent Viscosity	0.5-0.8	0.5-0.8	0.5-0.8	0.5-0.8	0.9-1.2	1.1-1.4
Melting Point (°C)	Amorphous	Amorphous	Amorphous	Amorphous	173-178	225-230
Glass Transition (°C)	45-50	45-50	50-55	55-60	60-65	35-40
Solubility	$MeCl_2$, THF, EtOAc, C_3H_6O	$MeCl_2$, THF, EtOAc, C_3H_6O	$MeCl_2$, THF, EtOAc, C_3H_6O	$MeCl_2$, THF, EtOAc, C_3H_6O	$MeCl_2$, $CHCl_3$	HFIP, HFASH
Tensile Strength (MPa)	41-55	41-55	41-55	28-41	55-83	69+
Modulus (MPa)	1379-2758	1379-2758	1379-2758	1379-2758	2758-4137	6895

[4] See URL: http://www.courses.ahc.umn.edu/medical-school/BMEn/5001/notes/bioabs.html Accessed 8.5.2004
[5] Specifications from Birmingham Polymers, Inc.

4 Materials, Apparatus, and Procedures

4.1 Electrode Design and Fabrication

In an effort to solve the mechanical and materials related issues previously described, a novel multi-electrode array was constructed. Formvar-insulated nichrome wire (25μm bare and 38μm coated diameter; A-M Systems) was cut to desired length with micro-dissecting scissors containing carbide inserts (4 ½", straight, sharp points, 25mm blades; Biomedical Research Instruments). This type of wire was chosen because it had already been successfully employed in neuronal recording. The insulation from one end was removed using a brief flame; stainless steel hypodermic tubing (Small Parts, Inc.) was used to protect the remainder of the wire. The non-insulated end was attached to a soldercup on a plastic shell circular electronic connector (12-socket with soldercups; Omnetics Connector Corporation) using high purity silver conductive paint (Structure Probe, Inc.). Although there are micro-connectors with a higher number of connections that are also more densely packed, this connector was chosen for its circular shape which allows an electrode bundle to be more easily fabricated. The specifications of the electronic connector are shown below (Figs. 5 and 6). This process was repeated twelve times until each soldercup was attached to a nichrome wire.

The quality of the wire-soldercup connections was checked using an electrode impedance meter (Model IMP-1; Bak Electronics, Inc.). A connection was deemed adequate if the impedance range fell between 0.5 – 2MΩ at 1 kHz. A multi-meter was also used to check for cross-connectivity between likely wire pairs. After the wire-soldercup connections were verified, the wires were tied together literally at a point just beyond the soldercups using a strand of fine wire. Then, the soldercups were coated with electrical potting compound (Loctite E-60NC Hysol; Loctite Corporation) up to where the wires converged into a single close-packed bundle and left to cure for twenty-four hours. Care was taken to prevent tangling or deforming the wires during the potting process.

The electrode bundle was either trimmed before or after polymer application; this affected the tip properties which will be discussed in the following section. The polymer was coated onto the electrode bundle using a solvent casting method. 50/50 poly(DL-lactide-co-glycolide) (inherent viscosity: 0.59dL/g in HFIP @ 30°C; Birmingham Polymers, Inc.) was dissolved in chloroform-D (Isotope D, 99.8%; Cambridge Isotope Laboratories, Inc.); typically, 0.4 grams of polymer was dissolved into approximately 4mL of chloroform. The electrode bundle was slowly dipped end on into the solution until the polymer coated up to the electrical potting compound and then removed. It is important to emphasize that the chloroform had a high vaporization rate; therefore, extra chloroform may have been added to prevent the solution from becoming too viscous for smooth coating. Any polymer that coated the electrode bundle unevenly would be removed by dipping the bundle back into chloroform. After the electrode bundle was smoothly coated, it was placed into a vacuum chamber (Nalgene; VWR International) for 24 hours to leach out the remaining solvent.

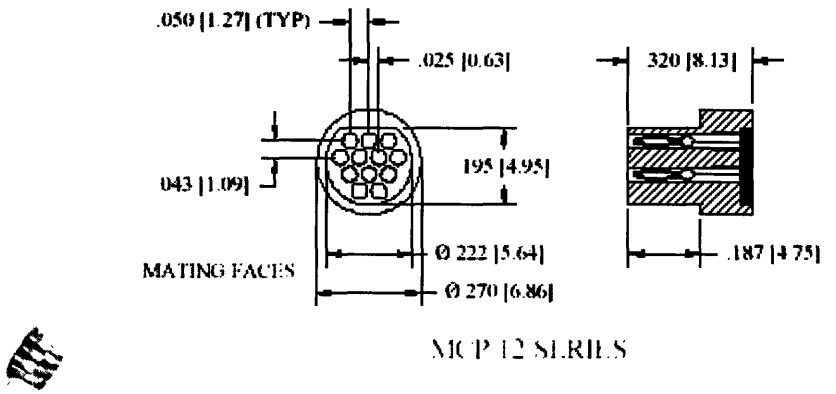

Figure 5. Twelve-socket male connector with soldercups from Omnetics Connector Corporation.[6] Number outside bracket is in inches and inside bracket is in millimeters. Each soldercup (shown as a small circle) is fixed to one Formvar-insulated nichrome wire. The male connector fits into a female pin connector that is attached to lead wires.

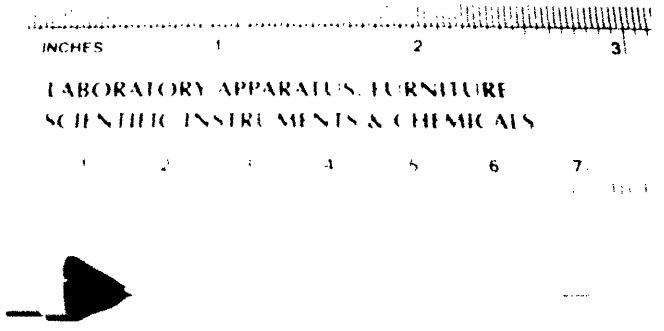

Figure 6. 12-electrode array with Omnetics connector. Black material is electrical potting compound. The wire bundle has already been coated with a bioerodible polymer.

4.2 Electrode Tip Design

One of the most significant aspects of electrode construction is the tip design. Electrodes made at present by the DiCarlo lab contain tips that have been electrochemically etched with sodium cyanide; these tips are approximately 1μm in diameter. Since each electrode wire in this multi-electrode array is approximately 30μm in diameter, the overall electrode bundle can have a diameter up to 120μm depending on the stacking arrangement. This is much wider than a typical electrode tip, and it has been hypothesized that such a large probe tip will push neurons away as

[6] See URL: http://www.omnetics.com/products/plasticmetalshell.html Accessed 8.1.2004

it separates brain tissue. A tip much smaller in diameter theoretically will have a better chance of advancing close to intact or healthy neurons without damaging tissue along the way.

We experimented with flat cut tips to study this hypothesis; a flat cut involved cutting the polymer coated bundle so that all electrode wires were of equal length. The probe tip diameter was the same as the rest of the shaft. Care was taken to ascertain that the cut was clean, and the impedances of the wires did not change from the cut. We also hoped to fashion the tip in a manner that maximized the number of different neuronal signals we could hear and record from. Several tip designs were experimented with and compared: angle cut, flat cut with splaying, and individual wire cut with splaying (Table 4). The first method involved cutting a dried coated bundle at a 45-60° angle. Each electrode wire would extend a different length from the bundle, allowing them to hopefully contact different neurons.

The second method consisted of flat cutting a dried coated bundle and dipping the bundle into chloroform to remove polymer a given distance from the tip. Removing polymer from the tip was termed splaying and would hopefully allow the wires to separate and spread outwards from the polymer fixed bundle. The distance and length of time taken to remove the polymer was varied to determine the conditions that yielded the optimal recording tip. In order to rapidly assess the quality of polymer removal, the study was performed initially using electrode wire bundles that were not wired to an electronic connector. After several promising conditions were determine, actual electrode bundles were fabricated using those conditions and tested. Splaying was performed by using a micro-manipulator to hold the electrode bundle and to lower it into a beaker containing chloroform. Contact was made when the electrode bundle created a small meniscus on the surface of the solvent; then the electrode was lowered into the liquid down to the desired depth.

Table 4 Fabrication Parameters for Optimization of the Electrode Probe Tip

Type of Cut	Cut Before Coating	Cut After Coating	Polymer Coat	Splay Distance [mm]	Splay Time [min]
45-60° Angle	No	Yes	Yes	--	--
Flat	Yes	No	Yes	0.5	5
				1.0	5
				1.0	10
				1.5	10
				2.0	2
				2.0	5
Individual	Yes	No	Yes	2.0	5
				2.0	10

The third method required each wire to be cut individually before polymer coating. The distance between the shortest and longest electrode wire never exceeded 500μm. The bundle was polymer coated and then immediately re-dipped into chloroform to remove polymer from the tip. The time and distance the tip was submerged in the solvent were varied using conditions from the second method that yielded promising results.

An additional tip modification involved gold-plating the electrode wire cross-sectional areas whenever the impedances were too high (greater than 1.0MΩ). Gold-plating has been used successfully by other groups (Wilson et al., 2003; Wilson F et al., 2003). This was performed using a micro-stimulator (Pulsar 6bp-as; FHC) set to output a continuous 1V pulse and gold-plating solution (SPS 5355, non-cyanide; Sifco Selective Plating). The micro-stimulator was also attached to an electrode impedance tester (Model IMP-1, Bak Electronics, Inc.) so that the impedance could be monitored continuously. Individual electrode tips were plated until the impedances fell between 0.3-0.8MΩ.

4.3 Electrode Port Construction

A novel electrode port was specially designed to house the multi-electrode arrays and served several purposes. First, this port was permanently attached over a small craniotomy on the test animal's skull and acted as a docking station for the electrode arrays. This allowed relatively easy access to brain tissue without requiring a craniotomy surgery for every experiment. The electrode port also included a convenient method of attaching an electrode for chronic implantation and allowed removal of the electrode when deemed necessary. Lastly, the electrode port protected the implanted electrode from mechanical damage and the electronic connector from soiling agents over the time span the array was attached to the test animal. All of these components were machined using standard methods (no special tools) out of titanium to offer an inert, lightweight port high in mechanical strength.

The head chamber was composed of three pieces – the cylindrical implant, the hex insert, and the cap. The cylindrical implant was the only component that was physically and permanently attached to the test subject's skull (Fig. 7). The bottom face of the implant was beveled to partially match the curvature of the skull and to prevent the implant when positioned at an angle from applying pressure on the brain surface; this angle was also necessary to guide the electrodes towards the IT cortex. The undercut beneath the large cylindrical face was designed to grab onto the bone cement that would fix the implant onto the skull and prevent it from being pulled out of the implant site. We relied on the adherence between the bone cement and implant to prevent rotation of the device.

The outside of the large cylinder was threaded (not shown in Fig. 7) to attach the cap component of the device. The slots on the threaded surface were designed for cap set screws to latch on and prevent the cap from unscrewing. Four slots were designed into the device, although fastening two set screws would suffice. Extra slots were machined into the component because the orientation of the device would be unknown until implantation; thus, some slots may be easier to access than others. Once a set screw was locked into a slot, the cap would not be able to rotate. However, if the set screw did manage to loosen, it would still remain fixed in the slot and the cap would be unable to detach. The inside of this cylinder piece was threaded to fit the hex insert as well. The cylindrical implant also contained a through-hole in which the guide tube and the electrode could be inserted through to access brain tissue (Fig. 8).

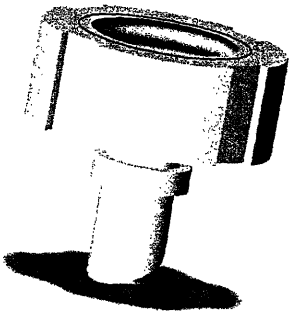

Figure 7. Cylindrical implant component of multi-electrode port; this piece was permanently fixed on the skull of the test subject. The beveled bottom of implant served to match the skull curvature and guide the electrode bundle towards the IT cortex region.

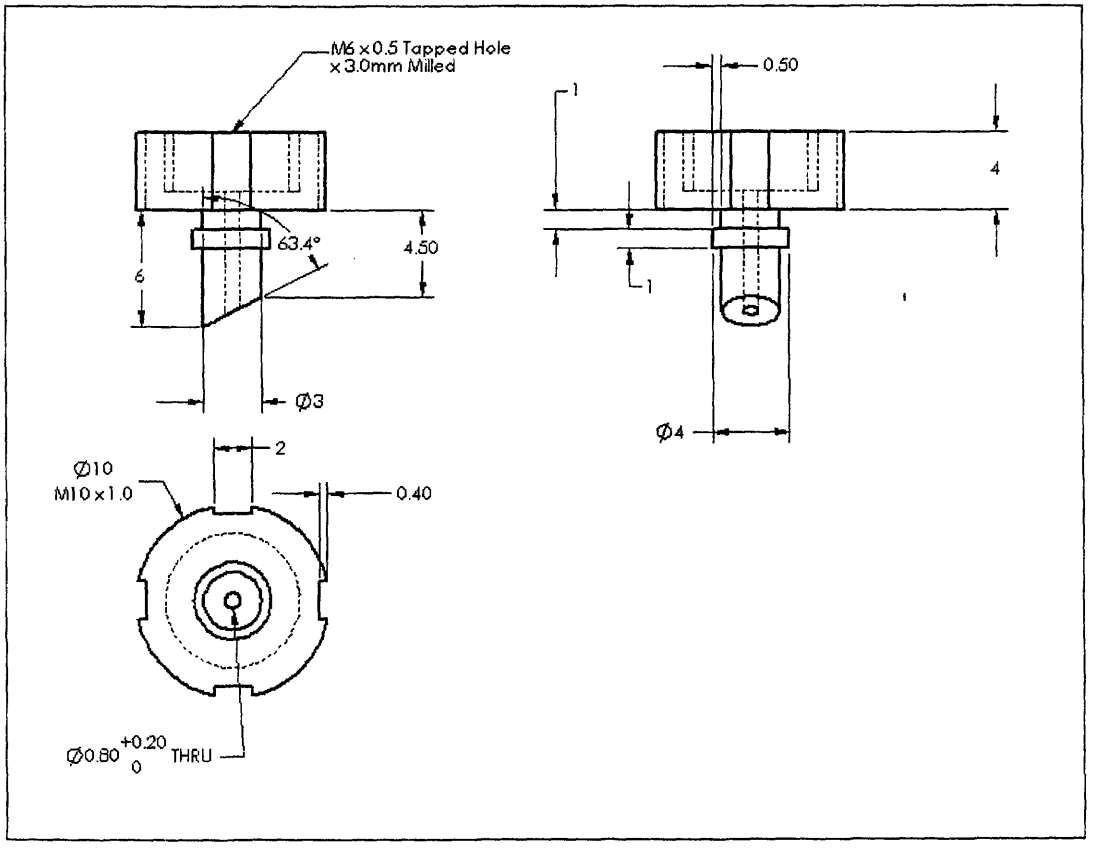

Figure 8. Schematic of the electrode port cylinder. The top two images represent side views of the cylinder; the bottom image is a top view. Dashed lines indicate the inner structure of the device. Dimensions are in millimeters and include specifications for machining the piece. This component was permanently implanted on the test subject's skull following a small craniotomy.

The second component of the electrode port was the hex insert. This piece served several purposes. A solid hex insert was used during surgery after the cylinder was implanted to act as an infection barrier. This prevented contaminants and infectious agents from migrating into the through-hole and then into the brain. A hollow hex insert was reserved for chronic implantation of a multi-electrode array. The electronic connector piece would be cradled in this hollow insert and would be fixed in place with bone cement. However, the electrode would still be removable because the insert could detach from the permanent cylindrical implant. One would need to remove the bone cement and slowly retract the electrode bundle from the brain. The hex insert could then be unfastened to clean off remaining residue.

The hex insert possessed a hexagonal face of accepted dimensions to allow easy tightening and loosening using standard nut drivers. The outside was threaded to match the inside of the cylindrical piece (Fig. 9). The large through-hole accommodated the guide tube, the electrode bundle, and part of the electrode connector (Fig. 10).

The final component of the electrode port was a titanium cap, which shielded the electronic connector from mechanical damage and weathering agents. The inside of the cap was partially threaded and matched the threads on the cylinder implant. Four threaded holes located near the bottom of the cap also acted as attachment points for the set screws (Fig. 11); the screws would penetrate through the cap to grab onto the wall of the cylinder implant.

The multi-electrode port components were optimized in scalability, limited only by the diameter and height of the electronic connector. Should higher density, more compact connectors become available on the market, the electrode array and subsequently the electrode port would be modified accordingly. The titanium walls on these pieces were also machined to be as thin as possible, approximately 1mm in thickness, while still providing sufficient mechanical rigidity. Overall, these new head chambers were much smaller than the ones currently used and a higher density of these ports on a skull could be accomplished.

Figure 9. Hexagonal-faced insert piece of multi-electrode port. This would attach to the chronic electrode array with bone cement and would serve for easy detachment of the electrode from the permanent port. Solid hex insert served as a barrier against infection during the pre-implantation period.

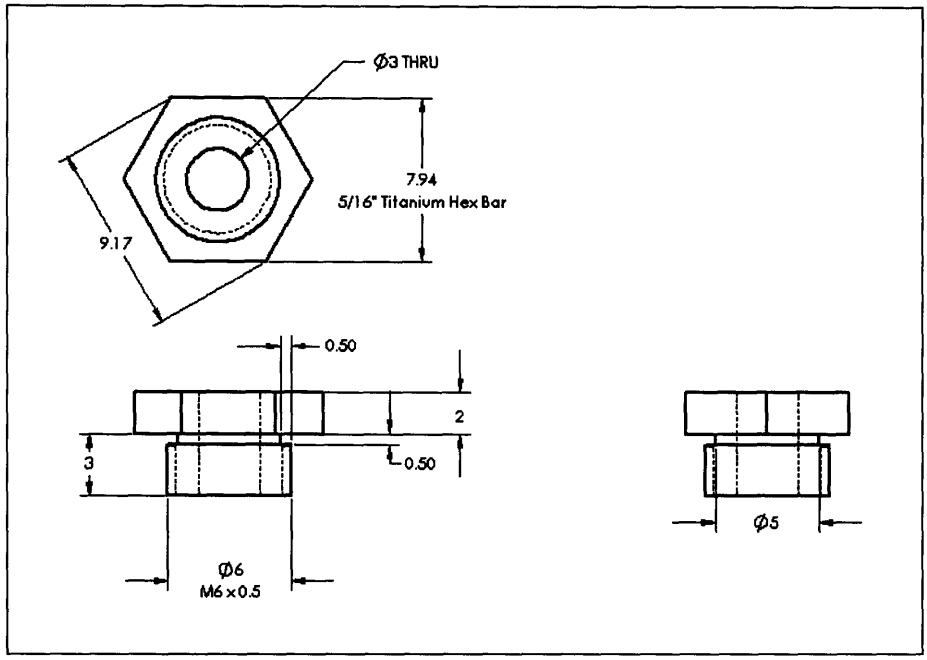

Figure 10. Diagram of the hexagonal-faced insert of the electrode port. The solid insert piece did not include the large 3mm through-hole as depicted in this schematic. The upper figure represents the top view of the component; the two bottom figures depict the side views. Dimensions are all in millimeters.

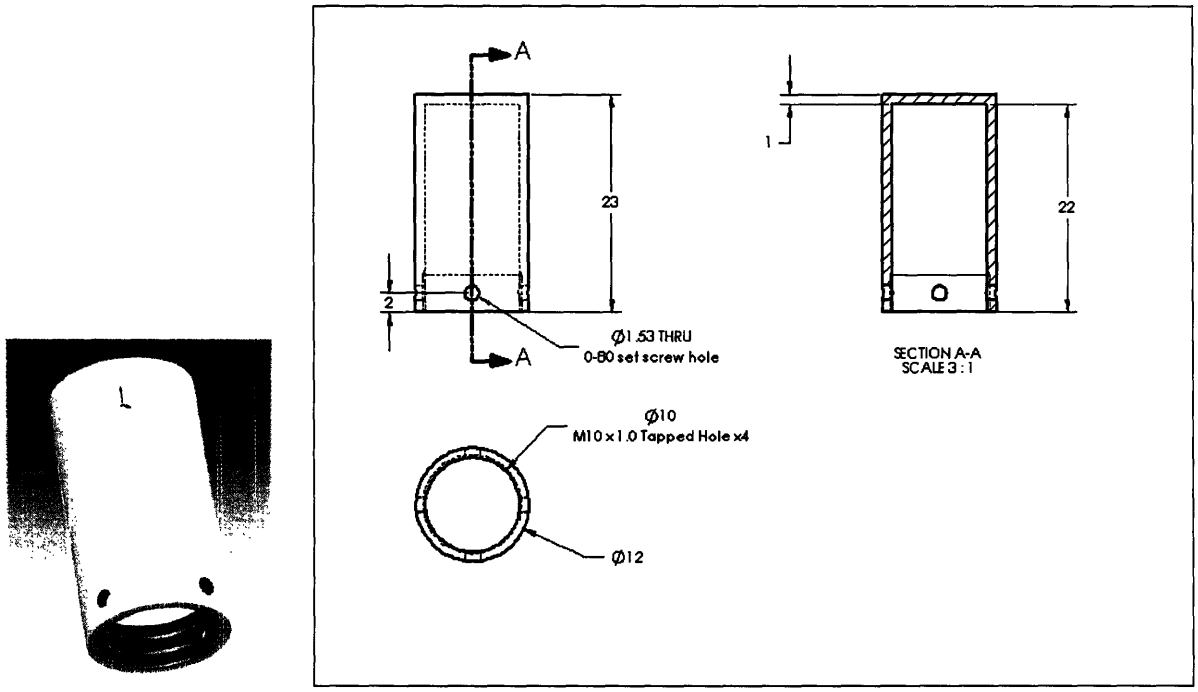

Figure 11. Rendering of titanium cap and schematic describing in millimeters the dimensions of the component. Four screw holes match up to the slots on the implant cylinder to prevent the cap from unscrewing.

4.4 Preliminary Testing with Existing Recording Platform

While the new electrode ports were designed and fabricated, preliminary testing of the multi-electrode arrays was conducted using the existing lab recording platform. Acute proof-of-concept experiments were performed to assess the quality and degree of neuronal signals that could be detected by these arrays. The main purpose was to temporarily insert these electrodes into brain tissue and record their performance. Different electrode tip designs were experimented with and evaluated as well.

The test subject was a male rhesus monkey (*Macaca mulatta*, 10.5 kg). Aseptic surgery had already been previously performed on the monkey to attach a head post for head fixation during visual experiments and a scleral search coil for monitoring eye movements. Following training in several visual tasks, a recording chamber was also attached in a subsequent surgery that required a small craniotomy. All procedures were conducted in accordance with NIH and MIT guidelines for animal experimentation and approved by the MIT Committee on Animal Care.

All recordings were made using multi-electrode bundles with an approximate diameter of 100μm that consisted of 12 nichrome wires each measuring 0.3-1.0MΩ in impedance. A number of tip designs were tested using this recording system – non-splayed flat cut, splayed flat cut, and non-splayed angle cut. Some of these electrodes were gold-plated as well to lower their impedance down to the desired range.

A guide tube 57.5mm in length (23 gauge; Small Parts, Inc.) was used to puncture dura and extend 20mm into the brain. This tube also aided the electrodes in reaching the IT area using a dorsal to ventral approach. The recording system was single-channel; only one electrode could be examined at a given time. Changing to different channels required manual switching. Neuronal spikes were amplified, filtered, and discriminated using standard equipment.

The electrode array was slowly lowered into the guide tube and brain tissue using an x-y-z adjustable stage (Crist Instruments Co., Inc.) and a standard electrode micro-drive (Kopf Instruments). Depth of the electrodes in the brain was continuously monitored and neuronal signal quality was assessed across different channels whenever possible.

4.5 Acute Testing using Multi-channel Recording System and Electrode Ports

Once the new electrode ports were manufactured and the multi-channel recording system was obtained, we tested the remaining electrode designs using a new procedure. The test subject for the chronically implanted electrode ports was a female rhesus monkey (*Macaca mulatta*, 3.8 kg). Aseptic surgery was performed to install a head post and a scleral search coil. Following several weeks of training on a fixation task (5-item rapid sequence), another surgery was performed to implant two electrode ports that pointed towards the bilateral IT cortex regions. All procedures were conducted in accordance with NIH and MIT guidelines for animal experimentation.

The acute experiments were conducted with multi-electrode arrays composed of nichrome wire electrodes with various tip designs – splayed flat cut, splayed individual cut, and non-splayed angle cut. A guide tube 20mm in length (23 gauge; Small Parts, Inc.) was used to puncture approximately 7mm into dura through the implanted titanium cylinder. The electrode bundle

was gradually lowered into the guide tube using an adjustable z-stage until it was 2mm inset. A standard electrode micro-drive (12-25μm/sec) was used to push the electrode into brain tissue. The stage and drive were attached to a goniometer (Thor Labs) and were positioned over the electrode port using a flexible support arm. The purpose of the goniometer was to allow finer adjustment along two tilt axes for more accurate positioning of the z-stage.

A 16-channel recording system (Plexon, Inc.) simultaneously observed all 12 electrodes in the array. Neuronal spikes were amplified, filtered, and discriminated through this system. Depth of the electrodes was constantly monitored and the quality of their recording properties was rapidly assessed throughout the experiment.

5 Results

5.1 Electrode Mechanical Properties

We evaluated whether the 12-electrode arrays possessed sufficient stiffness for brain insertion through acute experiments with the devices. Multiple trials of electrode insertion demonstrated that the arrays did not buckle during the advancement process into brain. A recording map of the electrodes overlaid with an MR image of a monkey brain determined whether the stiffness of the arrays was enough for it to track straight towards IT cortex (Fig. 12). This map was created from recording data generated from several experiments that indicated the depths at which neuronal signals were detected (Table 5). A depth of 0μm corresponded to approximately a 2mm inset of the array into the guide tube. The guide tube was estimated to penetrate 7mm into the brain.

Table 5 Data Generated from Angle Cut and Individually Cut Electrodes (-) = Nothing Heard

Depth [μm]	Angle cut / Non-plated Comment (Signal #)	Angle cut / Non-plated Comment (Signal #)	Individual cut / Plated Comment (Signal #)
0	-	-	-
1000	-	-	-
2000	-	-	-
3000	-	-	-
4000	faint cells (1)	cells (6)	-
4500	-	cells (2)	faint cells (5)
5000	-	-	-
5500	-	-	faint cells (3)
6000	faint cells (1)	cells (12,6)	-
6500	faint cells (11)	cells (12,6)	-
7000	some cells (6,7)	clear cells (2)	faint cells (4)
7500	small cells (6,7)	quieter	faint cells (5)
8000	-	-	-
8500	cell died (11)	cells (2)	cell (5)
9000	-	loud cells died (2,9)	cells (3,5)
9500	-	-	-
10000	-	-	cells (4,3)
10500	clear cells (11)	cells died (11)	cells (2)

Depth [µm]	Angle cut / Non-plated Comment (Signal #)	Angle cut / Non-plated Comment (Signal #)	Individual cut / Plated Comment (Signal #)
11000	cells (11)	cells died (11)	cells (2,1)
11500	-	cells died (11)	quieter
12000	-	cells (2)	cell died (2)
12500	-	-	-
13000	few cells	-	faint cells (2)
13500	-	-	cells (5,6,3)
14000	-	clear cells (2,11)	-
14500	cells (11)	cells died (6)	-
15000	distant cells (11)	clear cells (11)	-
15500	-	cells (11)	-
16000	-	loud cells (2,6)	cells died (5)
16500	distant cells (11)	loud cells (2,6)	cells died (5)
17000	-	loud cells (2,6)	cells died (5)
17500	-	cells died (11)	cells died (5)
18000	-	cells died (11)	loud cells died (5)
18500	clear cell (11,2,12)	-	loud cells died (5)
19000	cells died (11,2,12)	-	loud cells died (5)
19500	cells (11,2,12)	quieter	loud cells died (5)
20000	quieter	-	loud cells died (5)
20500	-	-	-
21000	distance cells (11)	-	-
21500	cells (11,6)	-	-
22000	cells died (11)	faint cells (2)	cell died (5)
22500	cells (11)	-	cells (5)
23000	cells (11)	faint cells (11)	-
23500	clear cells (11)	-	cells (5)
24000	clear crisp cells (1,5,6)	-	-
24500	-	-	cells (5)
25000	clear cells (11)	-	-
25500	-	cells died (11)	-
26000	distance cells (11)	cells died (11)	cells crackly (5)
26500	clear cells (11,5,6)	faint cells (11)	clear cells (5)
27000	clear cells (11)	-	-
27500	cells (11)	-	cell died (5)
28000	quieter	faint cells (2)	-
28500	cells (11)	-	-
29000	cells (11)	-	-
29500	cells approaching (11)	-	-
30000	-	-	-
30500	-	-	cells (5)
31000	-	-	cells (5)
31500		-	cells (5)
32000		-	-
32500		-	
33000		-	

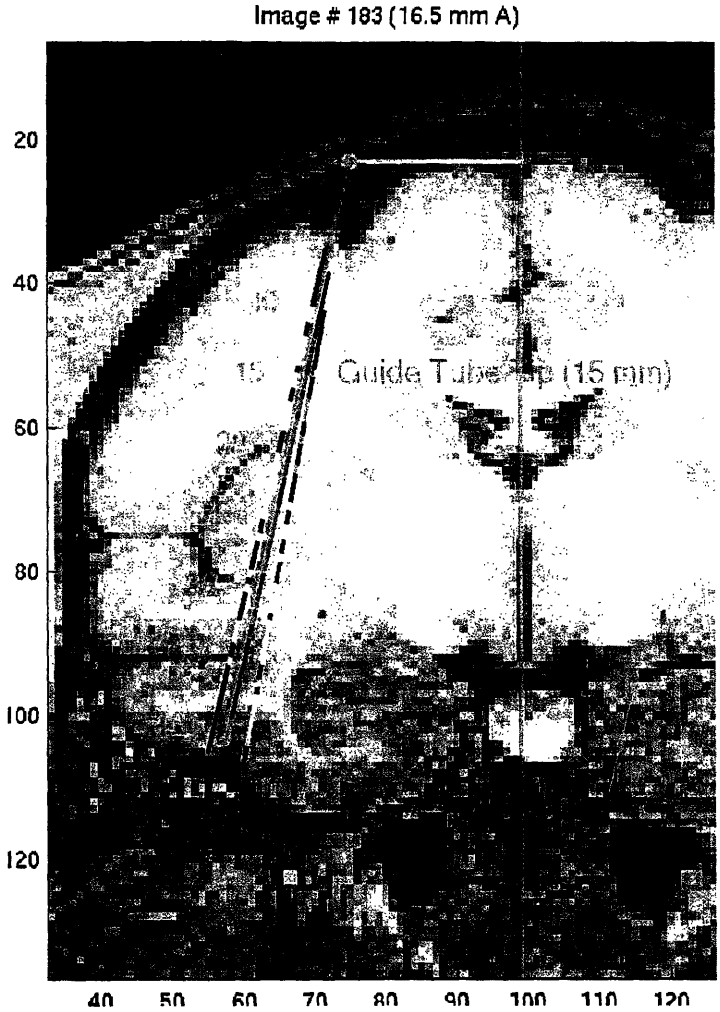

Figure 12. MR image of a non-human primate (chamber orientation = 12.7°) and overlay of the recording map obtained from several acute experiments. The lines represent the proposed directions of travel of each electrode based on their recording data – at what depths neuronal signals could be detected. Colored areas = neuronal signals detected. MR image courtesy of Davide Zoccolan (DiCarlo Lab).

The evidence given by acute experiments demonstrate that the multi-electrode arrays are stiff enough to insert into brain tissue and to track straight towards IT. However, to determine whether the electrodes truly become flexible they must be left implanted for a longer duration. The polymer was specifically selected for its ability to degrade upon contact with water. The D,L-PLA and PGA copolymer ratio as well as the molecular weight was tuned to provide the desired degradation rate. Given the evidence presented by literature for this polymer, we expect the polymer to degrade completely between 2-4 weeks after implantation. This can be confirmed by chronic recording experiments (see Section 6.4). Chronic implantation will not only determine the recording quality and stability of the electrodes during the polymer erosion process, but analysis of the array after it has been removed will reveal the degree of polymer degradation and whether original flexibility of the electrodes had been restored.

5.2 Surface Connection

Titanium electrode ports were successfully designed and constructed using standard machining techniques (Fig. 13). Created specifically for the 12-electrode arrays, the electrode port was much smaller than standard head chambers and thus much more scalable. Implantation of two ports on the skull of a non-human primate indicated that the dimensions and specifications for the device were accurate. Bone cement applied around the implant successfully secured the devices on the skull and prevented them from detaching. The right head chamber was permanently fixed and remained intact from the time of surgery until present (approximately 6-8 weeks). The left chamber, however, was able to rotate slightly after 4 weeks. We expected this when the bone cement used on that side during surgery had difficulty hardening. As a result, the top layer of bone cement was drilled off once the implant was discovered to be rotating, and new functional cement was applied to rectify the situation. This required using several threads that the cap fastened onto, and thus the cap was less secure on the implanted cylinder.

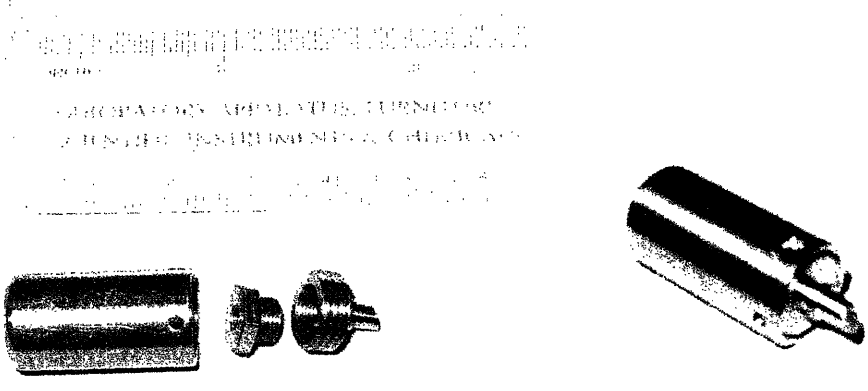

Figure 13. Electrode port composed of a cap, hex insert, and implant cylinder machined out of titanium. Two of these ports were implanted on the skull using bone cement and support screws. The fully assembled port is shown on the right.

5.3 Acute Recording Properties

To correlate the recording capabilities of the various electrodes to their tip designs, we first characterized each tip type through optical or fluorescence microscopy. We evaluated their recording capability based on how similarly it performed to a single stiff electrode. The tip design focused on removing as much polymer from the end of the electrode as possible, leaving approximately 0.5-2mm of free electrode wires. The fabrication parameters from Table 4 were tested and assessed.

The electrode bundles with 45-60° angle cuts composed of wires with distributed lengths. We hypothesized that the wires would contact neurons from different layers of brain tissue. The average distance between the shortest and longest electrode was 400μm. Since these arrays were cut after polymer coating, there was no residual polymer on the wire cross-sections, and the

electrode tips were very clean. Fluorescence microscopy (280nm, blue wavelength; 100x) was used to visualize the polymer between the electrodes and examine the wire stacking arrangement (Fig. 14). The polymer auto-fluoresced and is represented by the blue areas. Formvar insulation is depicted by the purple regions, and the dark circles are the nichrome wire cross-sections. There was no blue polymer on the nichrome tips, indicating that the electrodes were not contaminated with polymer and thus not impeded in recording capability.

The individually cut electrode arrays were also examined using fluorescence microscopy. The lengths of the electrodes were broadly distributed, but the average distance between the shortest and longest electrode was 375μm. The wire lengths and their stacking arrangement varied between each array as well, making the tip layout very difficult to duplicate (Fig. 15). These arrays were dipped under chloroform to remove polymer from the tip, but were not re-cut after coating. Thus, we examined whether polymer was deposited along the wire cross-sections, which would impede recording. In one bundle, the nichrome wires were clearly embedded in the blue fluorescing polymer. The longer electrodes were still clearly surrounded by polymer, even though chloroform was used to remove it from the tip. In the second array, one electrode extended much farther than the others and was not embedded in polymer. The shorter electrodes in that array were enveloped by the polymeric material. Due to the wide variation in electrode lengths, a single detailed picture of this entire electrode tip was difficult to obtain using this imaging technique. Although end-on views of the nichrome wire could not be achieved, the wire impedances were compared to un-coated electrodes, suggesting that at least part of the metallic tip was not covered with polymer.

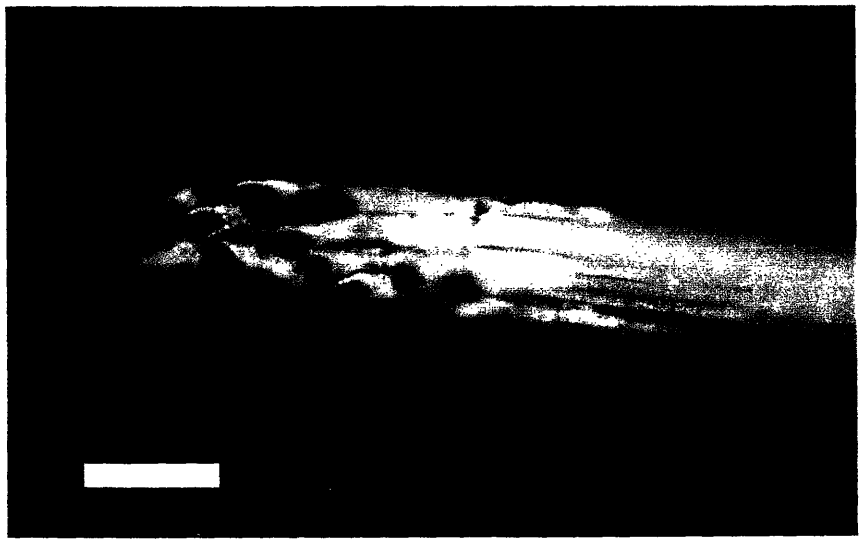

Figure 14. Fluorescence microscopy image of an angle cut multi-electrode tip (280nm, blue wavelength; 100x). The polymer auto-fluoresces and is indicated by the blue colored regions surrounding the wires, shown as the purple colored Formvar insulated areas with dark circular nichrome cross-sections. Bar = 120μm.

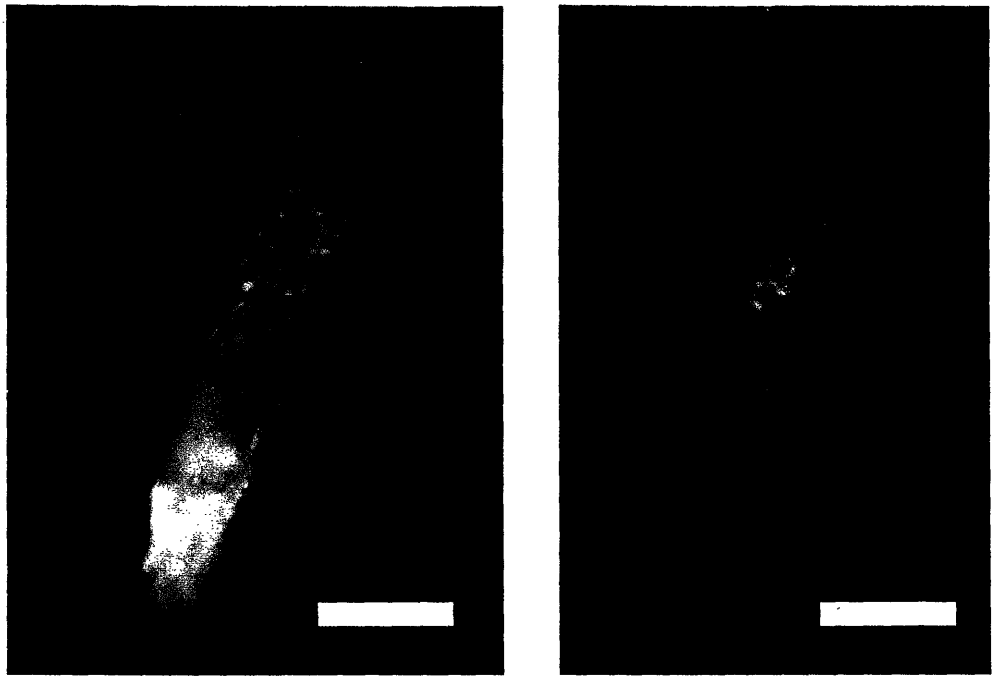

Figure 15. Fluorescence microscopy images of individually cut electrode bundles (280nm, blue wavelength; 100x). The left array is clearly embedded in the bioerodible polymer (blue), even the longest electrodes. The right array shows only polymer surrounding the shorter electrodes. Bar = 120μm.

The flat cut wire bundles were much more difficult to assess. Under an optical microscope at 40x, there was no clear distinction between polymer and free wire. A thinning of the coat could be easily visualized, but the electrode wires remained bonded to each other. We measured the distance the thinner coat extended from the tip. Applying a compressive force on the tip area also made only a few of the samples splay apart (Table 6). From this qualitative assessment, we determined that the bundles dipped 2.0mm into chloroform for at least 2-5 minutes were the most promising in having the tip separate into individual wires. This condition was used in the fabrication of the individually cut multi-electrodes. Fluorescence microscopy for this analysis was unavailable.

Table 6 Degree of Splaying in the Flat Cut Electrode Bundles Resulting from Dipping in Chloroform Solvent

Splay Distance [mm]	Splay Time [min]	Distance Thinner Coat Extended From Tip [mm]	Comment
0.5	5	1.25	Wires separated into clusters, but not individually
1.0	5	2.5	Individual wires did not split very well
1.0	10	2.5	Wires separated into clusters, but not individually
1.5	10	2.5	Wires separated into clusters, but not individually
2.0	2	4.0	Individual wires split from the bundle easily
2.0	5	4.0	Individual wires split from the bundle VERY easily

Many electrode variables were altered between the 13 acute experiments including gold-plating, tip construction, and the recording system used for gathering data. There was a great deal of variability in the results of these acute experiments. In the best experiments, multi-unit and single-unit isolations were detected at varying depths over 6-7 electrode channels. In the worst acute experiment, no neuronal signals were detected across all 12 channels during the entire course of the experiment. In the typical situation, distinct cells were heard at varying times across ~3 different channels.

- Effect of Gold Plating

The first two tests utilized un-plated non-splayed angle cut electrodes. These trials were unsuccessful because the impedances were too high, ranging from 0.9-2.3MΩ. Faint neuronal signals could be detected across five channels, but none that would be clearly defined as multi-unit activity or isolatable single-units. Overall, the electrode channels were too noisy to be able to discern neuronal signals from the background noise.

We also tested non-splayed plated flat cut electrode arrays. The gold-plating brought the impedances down to an acceptable range of 0.2-0.7MΩ. However, this type electrode did not perform well as it traveled down to a depth of 17,000μm, hearing nothing except vague neuronal signals along the way. An appropriate range of impedances was not the only critical factor for excellent recording quality, but the geometry of the electrode tip seemed to play an important role as well.

- Effect of Splaying

Tip geometry was altered by splaying the flat cut tips and was tested using both gold-plated and un-plated electrode arrays. The un-plated electrode bundle was much more successful than in previous trials with non-splayed flat cut or angular cut electrodes; this electrode bundle traveled 21,000μm deep and detected distinct neuronal signals across several channels. However, due to unresolved grounding issues with the recording equipment, there was difficulty in obtaining clearer signal quality.

Two trials of the gold-plated and splayed flat cut electrodes were evaluated. The first electrode array was splayed to such a degree that individual wires fanned out at the tip. The length that these wires were individually separated at the tip was 1.5mm and covered a circular area approximately 500μm in diameter. This large spread out tip caused difficulties when inserting the electrode into the guide tube. During the acute recording session, distinct neurons with eye-movement related responses were detected initially, but after driving only ~3000μm, no neuronal signals could be detected. Several electrode channels increased in impedance by over 0.5MΩ, indicative of a deformation in the wires or of organic material collecting on the tip. The multi-electrode array was also difficult to extract through the guide tube when it was withdrawn out of brain tissue.

The flat cut electrode splayed to a much lesser degree was superior to the previous electrode. The tip was dipped 1.5mm under chloroform for 10 minutes, but separation of the wires was not visibly apparent under an optical microscope (40x). Seven channels identified neurons at various

stages of electrode advancement to a depth of 7500μm; the impedance range of these channels was 0.2-0.7MΩ.

▪ Effect of Tip Cutting

Electrodes that were individually cut, coated, then splayed below 1.5mm of chloroform for 15 minutes produced significantly better results than the splayed flat cut electrodes. One channel with an impedance of 0.4MΩ performed exceptionally, detecting many isolatable single-units throughout insertion into the brain. This electrode array also advanced the farthest depth during that point in time, approximately 16,000μm into the brain.

Individually cut electrodes all gold-plated to 0.7MΩ and splayed in 2.0mm of chloroform for 10 minutes produced arrays with the best performance. In both trials, seven channels could hear multi-unit activity and on occasion isolatable single-units (Fig. 16). The signal quality was much more representative of a single stiff electrode. The maximum depth traveled was approximately 32,000μm; depth was confirmed through mapping of gray and white matter areas of the brain and comparison with existing brain scan images. The array was left at this depth for a period of 2 hours to determine if the signal quality would improve as the brain matter resettled itself. Over that period of time, multi-unit activity initially increased, but the quality of the neuronal signals gradually degraded. If the electrode array was advanced several hundred microns, however, multi-unit activity would re-appear.

The non-splayed un-plated angle cut electrodes tested almost as well, traveling down to a maximum depth of 31,000μm. Impedance of the electrodes ranged from 0.3-0.8MΩ. Six channels recorded multi-unit activity throughout the experiment. In these trials, the electrode arrays were also parked over a period of 2 hours. The same phenomenon as the individually cut electrodes occurred; multi-unit activity appeared initially, but disappeared over time. If the electrode array moved deeper into tissue, new multi-unit activity developed.

▪ Effect of Applying a Multi-channel Recording System (Plexon)

The tests using the existing single-channel recording platform were difficult to conduct; all 12 channels could not be simultaneously monitored during insertion of the electrode down to deep brain matter. Several trials were also unsuccessful due to technical problems with the equipment, which prevented a clearer signal output from the electrode devices. The arrays that did not encounter these issues were only tested across approximately six channels in each trial. The manual switching to different electrode channels proved to be quite challenging because at different depths there was no method to determine which channel was best suited for detecting neuronal signals. We focused only on the channels that showed an impedance range between 0.4-0.8MΩ; previous experience with stiff single electrodes indicated that this impedance range yielded the best signal quality.

The Plexon system allowed all 12 channels to be rapidly evaluated and continuously monitored as the electrode array advanced into deep brain tissue. Those with high impedances were examined as well and in general possessed higher noise than those with impedance in the range of 0.3-0.7MΩ. Since all 12 channels could be examined at once, determination of the most

promising electrodes was more informed. This system was far comprehensive in testing the arrays than the single-channel platform.

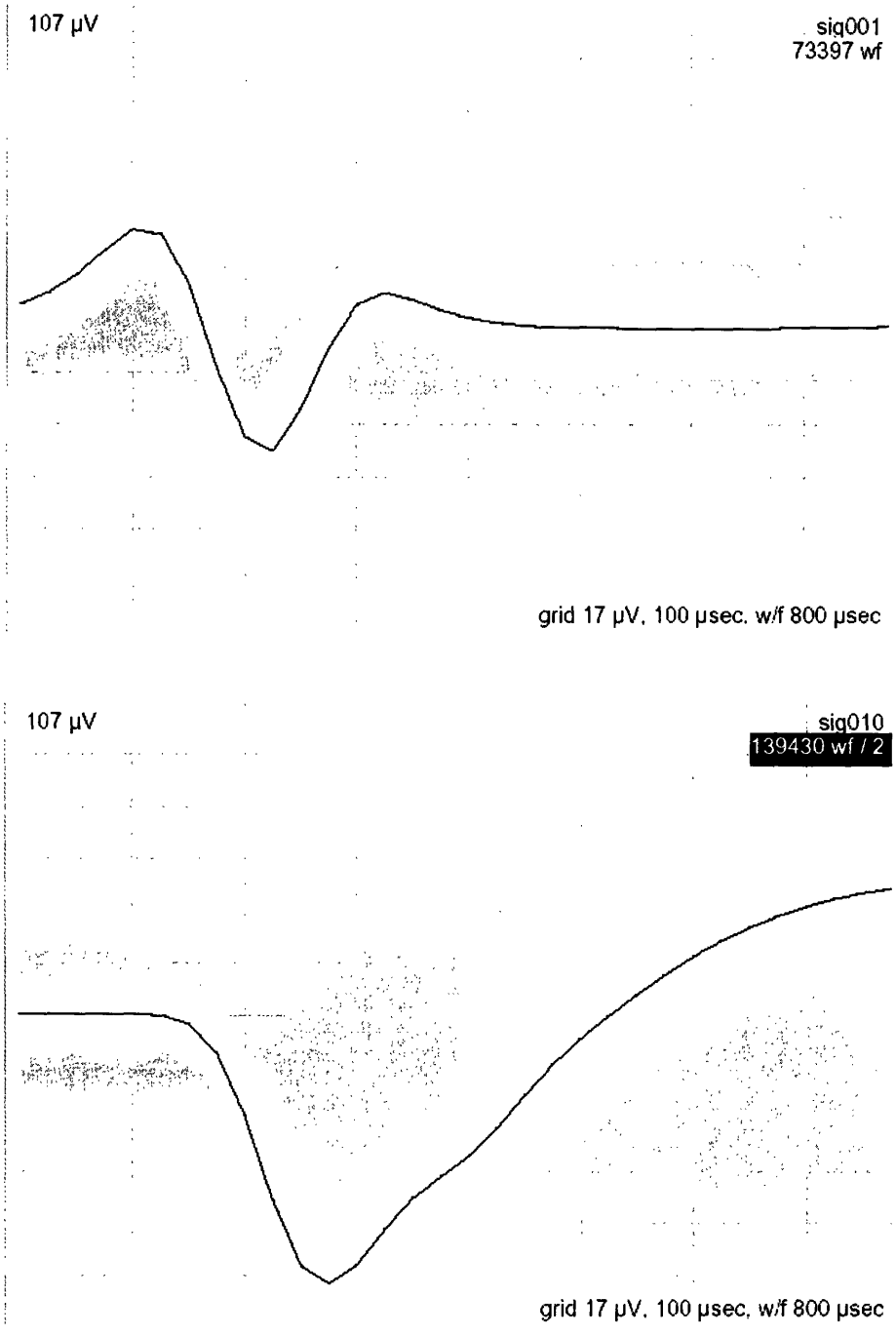

Figure 16. Multi-unit activity (yellow) detected from two different channels or electrodes during one trial using an individually cut electrode. The gray area is the background noise. The trough-to-peak amplitude of the waveform was approximately 110µV (top) and 153 µV (bottom). These images were generated using the off-line sorter on recorded Plexon data.

6 Discussion

6.1 Electrode Mechanical Properties

Although we learned that a 12-electrode array is sufficiently stiff to insert into the brain, it would be interesting to determine the minimum number of wires needed to penetrate brain tissue. What value does the critical load for buckling have to be in order for the electrode or electrode bundle to be resistant to buckling during insertion? The answer can be determined empirically through a series of acute experiments with electrode bundles that vary in the number of wires. Each bundle can be inserted into brain tissue and evaluated for its stiffness. Once the minimum number of wires is determined, we can also mathematically estimate the critical load for buckling possessed by that sample.

More comprehensive analyses of the electrode tip could also be performed in addition to qualitative compression tests. For example, an electromechanical Instron machine could be used to measure low cycle fatigue and run standard uniaxial tension/compression tests for small and thin specimens. As the polymer degraded over time, the splaying was also predicted to become more pronounced. The wires would be less restrained in the composite as the polymer eroded and thus would have more freedom to move around in tissue. It would be interesting to first determine whether the chosen polymer truly degraded in the desired time frame through several chronic experiments. Then, additional fluorescence microscopy imaging could be employed to characterize the degree of polymer breakdown at the tip, since ultimately this is where we would care the most about the polymer eroding.

6.2 Surface Connection

The electrode port implanted on the skull withstood mechanical forces that inevitably arose during the subject's daily activities in its home cage. The large lever arm of the titanium cap was particularly worrisome, especially since it could no longer be scaled down without changing the type of electronic connector used. While the titanium port remained fastened to the skull, there was a problem with one implant rotating very slightly. We initially assumed the friction between the bone cement and the implant, especially in the cylinder undercut, would be sufficient to hold the port. This was true for the right electrode port, but the left port could rotate for several reasons. The slightly loose electrode port was implanted over a much larger craniotomy, and the bone cement may not have been optimal strength as there was some variability in the preparation process. It may be beneficial to add vertical slots in the undercut of the second generation implant to increase the grab between the cement and titanium.

6.3 Acute Recording Properties

Characterization of the numerous electrode tip designs and evaluation of their recording capability led to several conclusions. Electrode wire impedances that fell between 0.3-0.7MΩ demonstrated the best recording quality. Higher impedances resulted in noisy signals, which multi-unit or single-unit activity was difficult to isolate from. Lower impedance electrodes were unable to detect signals and were silent throughout. Flat cut electrode arrays also performed worse than angle cut or individual cut arrays. We hypothesized that this was because the large electrode bundle separated tissue and pushed away neurons during insertion into the brain. Electrode tips of typical sharp electrodes are much smaller in diameter, approximately 1-5μm.

These electrode arrays, however, were blunt tipped and thus the diameter was the same as the rest of the bundle. The tip could be as large as 120μm and would be two orders of magnitude larger than the current single stiff electrode tips.

The results from the angle and individual cuts supported this theory; both tip designs were clearly superior in recording capability compared to the flat cut arrays. Multi-unit activity and isolatable single-units were detected on seven channels at various depths. The electrode lengths varied in each array, and the distance between the longest and shortest electrode was approximately 400μm. We conjectured that this allowed individual electrodes to contact different neurons without significant tissue displacement. Angle cut electrodes possessed a slanted tip that likely slipped easily near cells as well.

Splaying also seemed to improve electrode recording. Fluorescence microscopy indicated that residual polymer was still present at the tip despite attempted removal using chloroform. This was further confirmed by difficulty in separating the tips when compressive force was applied. However, electrode arrays with tips that remained bonded to each other performed well during recording. It would be worthwhile to further investigate the degree of splaying that would provide the optimal recording conditions – how much polymer should be removed and at what length from the tips? To better remove the polymer, the chloroform could also be agitated, unlike our splaying tests when the electrodes were simply submerged under stagnant solvent. For example, an ultrasonic homogenizer could be applied to agitate the solvent and accelerate the polymer dissolving process.

Although separation of the tips would result in a higher chance of contacting different neurons, we also recognized that over-splaying could be potentially disadvantageous during the insertion process. The electrode bundle, splayed until all wires were separated, resulted in a tip that was much larger than the bundle itself. This was difficult to insert into the guide tube and had very poor recording quality beyond a depth of 5000μm. We hypothesized that the wires had insufficient mechanical stiffness individually to withstand flexing during insertion into tissue. The electrodes had good recording properties when they first entered the tissue, but as the electrode advanced the impedance increased and recording capability became very poor. We conjectured that the wires curled back up against the bundle as the array advanced, thus permanently bending the wires and causing the impedances to increase. This was supported by the difficulty in retracting the electrode from the guide tube at the end of the experiment. It was unlikely that the impedances increased from organic material collecting at the tip; the increase in impedance occurred much too quickly from traveling only 5000μm. The degree of splaying in this case was certainly not optimal. If the electrode tips curled back towards the bundle, it would damage brain tissue as it advanced into and retracted from the brain. Furthermore, the tips would buckle and be unable to detect neuronal signals. The electrode tips would also have a higher chance of breaking off as a result of the mechanical stress.

In the recording trials thus far, only a maximum of seven electrodes had been active over the course of an experiment. This may largely have been due to tip design; longer electrodes were individually exposed and not enclosed by other electrodes. Shorter electrodes were nested within individually cut bundles and isolated away from neurons. Angle cut electrodes, however, did not

support this theory. Experiments conducted using angle cut arrays also did not yield more than seven active channels. These electrode tips were all exposed and did not obstruct one another. More experiments would determine whether only a limited number of electrodes would be active at one time or if all twelve electrodes in an array would be capable of recording. However, we did observe that, in general, electrodes that were active during the beginning of electrode insertion remained active as the array was driven deeper toward our target. Those that detected no neuronal signals continued to be silent throughout the duration of the trial.

Gold-plating the electrodes helped to lower the impedance. However, not all electrodes needed to be plated, and if the impedance was similar, plated and un-plated electrodes recorded equally well. We expected that depositing a thin gold layer would not impair the electrode or change the electrode tip geometry. However, electrodes that possessed unusually high impedance brought down by gold-plating still seemed to have poor recording quality. This may have been the result of the plating changing the tip geometry; such a large amount of gold was needed to decrease the impedance down to an acceptable value that it was no longer added on as a thin layer. Fluorescence microscopy or some other imaging technique should be used to characterize the electrode tips after gold-plating to determine whether there was a change in tip geometry.

6.4 Chronic Recording Properties

The experiments indicated that leaving the electrode arrays at a depth between 31,000-32,000μm for 2 hours did not result in better recording quality. The electrodes would detect additional neuronal signals at first, but would gradually lose them over time. We hypothesized that initially the brain tissue slowly moved past the electrode tip to relax the compression induced by electrode advancement. This was represented by the delayed neuronal signals detected by the electrode. However, the array would settle in an area that was not particularly active. Experiments run for a longer duration would further elucidate the premises behind this phenomena. The electrodes may have rested for an insufficient amount of time; it may take much longer than two hours before the brain tissue fully resettles. Indeed, some studies with other electrode designs suggest that several days or more are required to reach optimal recording (Eric Jonas, Personal communication). Chronic experiments that are currently underway will aid in determining how long the electrode array developed here must remain implanted for neuronal recording to stabilize. Our next aim would be to implant an electrode device for several months and to observe this trend. These chronic experiments can also reveal the true polymer degradation characteristics and whether removing polymer from the tip (splaying) can improve recording quality and/or stability.

7 Conclusion

The primary aim of this project was to create a multi-electrode array that was stiff during insertion and flexible after implantation. A compact 12-electrode array was designed, fabricated, and tested for stiffness through acute experiments. We determined that this polymer coated flexible wire bundle was satisfactorily stiff and did not buckle during advancement into tissue. Using the MR images and the recording map overlay, we also demonstrated that the electrode tracked reasonably straight towards IT. As for the array becoming more flexible during implantation through polymer erosion, only chronic tests where the electrodes are implanted for

long periods of time (weeks or months) will reveal whether this is true. Data from literature suggests that for bioerodible 50/50 poly(D,L-lactide-co-glycolide), the degradation time based on the array size and geometry will be between 2-4 weeks. To our best knowledge thus far, the intrinsic flexibility of the individual electrodes will be restored after that period of time.

Our second aim of designing, constructing, and implanting novel electrode ports that house the arrays had been successful. Its durability was tested and evaluated, and a second generation prototype will subsequently be designed to include new characteristics (such as 1-2mm of electrode travel). Multiple ports will be implanted on a new test subject. For now, the two electrode ports are sufficient for testing the electrodes. Currently, one electrode port is used for acute experiments while the second port is reserved for chronic implantation. The multi-channel Plexon system assists in rapid assessment of each electrode device, and the length of each experiment is drastically reduced.

The third aim involved testing electrodes that were varied in a whole range of parameters such as gold-plating, splaying, final tip cut, and recording platform through a series of acute experiments. The results indicated that electrode tip construction and recording capability were strongly interlinked. The impedance range must fall between 0.3-0.8MΩ for good neuronal signal detection. The best recording, which was 6-7 active channels that detected multi-unit and sometimes isolatable single-unit activity, was performed by angle and individually cut electrodes. Splaying or removing polymer from the electrode tips also improved the recording quality, but to what degree remains to be determined. Chronic implantation of these electrodes will also reveal whether the signal quality and stability of the arrays improve or worsen with time. These experiments are currently underway and will involve 1-2 months of recording. Our long-term goal is to expand this into a fully chronic device, which eventually we can leave implanted for 6 months to 1 year.

Acknowledgements

I wish to express my gratitude to Professor James DiCarlo for his endless support and for carefully supervising my M.Eng. work. I thank David Cox for his beneficial scientific suggestions and helpful comments throughout my project. The time that he spent helping me with the acute recording experiments was invaluable. I also wish to thank all my colleagues in the DiCarlo lab and am especially grateful to Davide Zoccolan, Chou Hung, and Jennifer Deutsch.

References

Aronov D, Reich DS, Mechler F, Victor JD. Neural coding of spatial phase in V1 of the macaque monkey. J Neurophysiol 2003; 89: 3304-3327.

Emerich DF, Tracy MA, Ward KL, Figueiredo M, Qian R, Henschel C, Bartus RT. Biocompatibility of poly (DL-lactide-co-glycolide) microspheres implanted into brain. Cell Transplant 1999; 8: 47-58.

Erickson CA, Desimone R. Responses of macaque perirhinal neurons during and after visual stimulus association learning. J Neurosci 1999; 19: 10404-10416.

Fournier E, Passirani C, Montero-Menei CN, Benoit JP. Biocompatibility of implantable synthetic polymeric drug carriers: focus on brain biocompatibility: Review. Biomaterials 2003; 24: 3311-3331.

Gray CM, Maldonado PE, Wilson M, McNaughton B. Tetrodes markedly improve the reliability and yield of multiple single-unit isolation from multi-unit recordings in cat striate cortex. J Neurosci Methods 1995; 63: 43-54.

Jeantet Y, Cho YH. Design of a twin tetrode microdrive and headstage for hippocampal single unit recordings in behaving mice. J Neurosci Methods 2003; 129:129-134.

Kou JH, Emmett C, Shen P, Aswani S, Iwamoto T, Vaghefi F, Cain G, Sanders L. Bioerosion and biocompatibility of poly(*d,l*-lactic-co-glycolic acid) implants in brain. Journal of Controlled Release 1997; 43: 123-130.

Mechler F, Reich DS, Victor JD. Detection and discrimination of relative spatial phase by V1 neurons. J Neurosci 2002; 22: 6129-6157.

Miller RA, Brady JM, Cutright DE. Degradation rates of oral resorbable implants (polylactates and polyglycolates): rate modification with changes in PLA/PGA copolymer ratios. J Biomed Mater Res 1977; 11: 711-719.

Nicolelis MA, Dimitrov D, Carmena JM, Crist R, Lehew G, Kralik JD, Wise SP. Chronic, multisite, multielectrode recordings in macaque monkeys. Proc Natl Acad Sci 2003; 100: 11041-11046.

Porada I, Bondar I, Spatz WB, Krüger J. Rabbit and monkey visual cortex: more than a year of recording with up to 64 microelectrodes. J Neurosci Methods 2000; 95: 13-28.

Ratner BD, Hoffman AS, Schoen FJ, Lemons JE. Biomaterials Science: An Introduction to Materials in Medicine. Elsevier Science: 1996.

Williams DF. Some observations on the role of cellular enzymes in the *in vivo* degradation of polymers. In: Syrett BC, Acharya A, editors. Corrosion and degradation of implant materials. 1979. pp.61-75.

Williams DF. Definitions in Biomaterials. Proceedings of a Consensus Conference of the European Society for Biomaterials, Chester, England, March 3-5 1986, Vol. 4, Elsevier, New York.

Wilson F, Ma Y, Greenberg PA, Ryou JW. A microelectrode drive for long term recording of neurons in freely moving and chaired monkeys. J Neurosci Methods 2003; 127: 49-61.

Wilson M, McNaughton B. Dynamics of the Hippocampal Ensemble Code for Space. Science 1993; 261:1055-1058.

Veziers J, Lesourd M, Jollivet C, Montero-Menei C, Benoit JP, Menei P. Analysis of brain biocompatibility of drug-releasing microspheres by scanning and transmission electron microscopy. J Neurosurg 2001; 95: 489-494.